AD-A126 866 HIGH ANGULAR RESOLUTION MICROWAVE SENSING WITH LARGE SPARSE RANDOM ARRAYS..(U) MOORE SCHOOL OF ELECTRICAL ENGINEERING PHILADELPHIA PA VALLEY.. C N DORNY ET AL. 1/1

UNCLASSIFIED DEC 82 UP-VFRC-29-82 AFOSR-TR-83-0225 F/G 17/9 NL

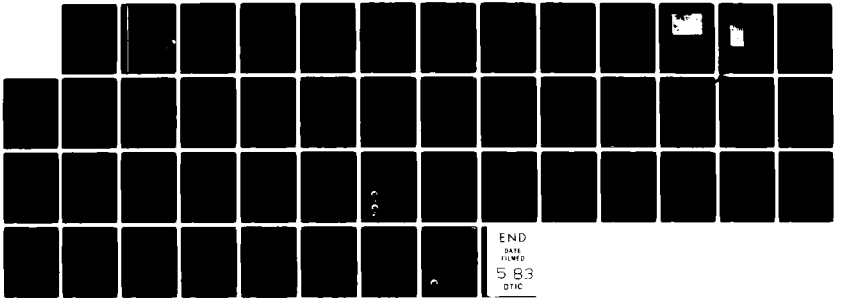

END
DATE FILMED
5 83
DTIC

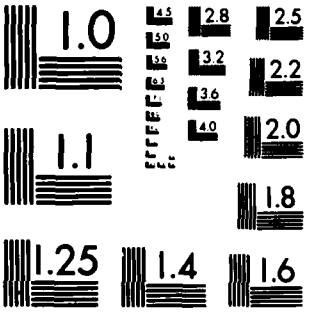

HIGH ANGULAR RESOLUTION MICROWAVE SENSING WITH LARGE, SPARSE, RANDOM ARRAYS

Annual Technical Report

to

AIR FORCE OFFICE OF SCIENTIFIC RESEARCH

AFOSR 82-0012

UNIVERSITY of PENNSYLVANIA

VALLEY FORGE RESEARCH CENTER

THE MOORE SCHOOL OF ELECTRICAL ENGINEERING

PHILADELPHIA, PENNSYLVANIA 19174

UP-VFRC-29-82

December 1982

HIGH ANGULAR RESOLUTION MICROWAVE SENSING WITH LARGE, SPARSE, RANDOM ARRAYS

Annual Technical Report

to

AIR FORCE OFFICE OF SCIENTIFIC RESEARCH

AFOSR 82-0012

Valley Forge Research Center
The Moore School of Electrical Engineering
University of Pennsylvania
Philadelphia, Pennsylvania 19104

ABSTRACT

This document describes progress toward development of a general capability for high resolution microwave surveillance and imaging using large, sparse, self-cohering arrays. During the last year progress has been made in unification of self-cohering techniques, and in development of techniques for reducing the effects of the high sidelobes associated with sparse arrays.

UNCLASSIFIED

SECURITY CLASSIFICATION OF THIS PAGE (When Data Entered)

REPORT DOCUMENTATION PAGE	READ INSTRUCTIONS BEFORE COMPLETING FORM
1. REPORT NUMBER **AFOSR-TR- 83-0225** 2. GOVT ACCESSION NO. AD-A126 86	3. RECIPIENT'S CATALOG NUMBER
4. TITLE (and Subtitle) HIGH ANGULAR RESOLUTION MICROWAVE SENSING WITH LARGE, SPARSE, RANDOM ARRAYS	5. TYPE OF REPORT & PERIOD COVERED Annual Technical Report 1 Oct 81 - 30 Sept 82
	6. PERFORMING ORG. REPORT NUMBER UP-VFRC-29-82
7. AUTHOR(s) C. Nelson Dorny Bernard D. Steinberg	8. CONTRACT OR GRANT NUMBER(s) AFOSR-82-0012
9. PERFORMING ORGANIZATION NAME AND ADDRESS Valley Forge Research Center, Moore School of Electircal Engineering, University of Pennsylvania Philadelphia, PA 19104	10. PROGRAM ELEMENT, PROJECT, TASK AREA & WORK UNIT NUMBERS 2305/B1 61102F
11. CONTROLLING OFFICE NAME AND ADDRESS Air Force Office of Scientific Research/NE Building 410, Bolling AFB, D.C. 20332	12. REPORT DATE December 1982
	13. NUMBER OF PAGES 12 not counting attachments
14. MONITORING AGENCY NAME & ADDRESS(if different from Controlling Office)	15. SECURITY CLASS. (of this report) Unclassified
	15a. DECLASSIFICATION/DOWNGRADING SCHEDULE N/A

16. DISTRIBUTION STATEMENT (of this Report)

Approved for public release;
distribution unlimited.

17. DISTRIBUTION STATEMENT (of the abstract entered in Block 20, if different from Report)

18. SUPPLEMENTARY NOTES

19. KEY WORDS (Continue on reverse side if necessary and identify by block number)

20. ABSTRACT (Continue on reverse side if necessary and identify by block number)

This document describes progress toward development of a general capability for high resolution microwave surveillance and imaging using large, sparse, self-cohering arrays. During the last year progress has been made in unification of self-cohering techniques, and in development of techniques for reducing the effects of the high sidelobes associated with sparse arrays.

DD FORM 1 JAN 73 1473 EDITION OF 1 NOV 65 IS OBSOLETE

UNCLASSIFIED

SECURITY CLASSIFICATION OF THIS PAGE (When Data Entered)

TABLE OF CONTENTS

HIGH ANGULAR RESOLUTION MICROWAVE SENSING WITH LARGE, SPARSE, RANDOM ARRAYS

RESEARCH OBJECTIVES

The long-term objective of this research program is the development of a general capability for high resolution microwave surveillance and imaging. Fundamental to such a general capability is the ability to cohere large, poorly surveyed possible flexing microwave arrays. Some form of adaptivity, referred to in this document as self-cohering, is required in order to form high quality beams with such arrays.

The specific objectives of the program are:

1. To expand understanding of self-cohering arrays in a broad range of applications.

2. To understand the effects of multipath and other propagation phenomena on the operation of large, self-cohering arrays; to devise system concepts for minimizing the degrading effects of such propagation irregularities.

3. To understand the effects of jamming and other interference phenomena on the operation of large, self-cohering arrays; to devise system concepts for minimizing the degrading effect of these interference phenomena.

4. To devise spatial and temporal signal processing techniques which optimize the beam characteristics of large, self-cohering arrays in the presence of noise, interference, multipath, and other degrading phenomena.

5. To design and perform experiments to test the models, system concepts, and theories developed in 1 through 4.

STATUS OF THE RESEARCH EFFORT

Prior to the initiation of AFOSR support, two techniques for self-cohering were developed which use information external to the array (beacon signals or target reflections) to aid in beamforming. Both of these self-cohering concepts have been verified experimentally (at L-band) at our Valley Forge Research Center test range.

During the first three years of support by AFOSR, program effort was focused on enhancing self-cohering capability, development of spread spectrum and nulling techniques for reducing the effects of interference on self-cohering of real and synthetic apertures, modelling the effects of multipath on self-cohered beams and experimental verification of these models, and on the development of advanced system concepts (ground-based, airborne, and space-based radio cameras and forward-looking synthetic aperture radar), on refinement of our self-cohering techniques compatible with those system concepts, on hardware testing of self-cohering techniques, and on the development of methods for enhancing the quality of microwave images obtained through large, sparse arrays [1-3].

During the past year work has continued on experimental imaging and data base development, on broadening of self-cohering capability, and on image quality improvement. The present focus of the research effort is directed primarily toward image quality improvement in very sparse, random microwave imaging systems, toward a study of the feasibility of large, sparse, random apertures using multiple vehicles, and toward unification of self-cohering concepts.

Advantages of Large Self-Cohering Arrays

Extended study of the applicability and advantages of large self-cohering arrays for a broad range of applications has discovered the following potential advantages associated with those arrays:

1. Improvement in the range/power trade off in radar and communications as a result of the high power-aperture product (owing to large size).
2. Improvement in resolution and tracking (or pointing) accuracy owing to small beamwidth associated with large arrays.
3. Lowered probability of intercept and improved interference rejection in communications, direction finding, and radar owing to the small beamwidth associated with large arrays, and owing to the high degree of null control associated with individual-element phase control. Adaptively placed nulls can track moving interferers and ease sidelobe level requirements.

4. Extension of the capability for high resolution searching and imaging in either monostatic or bistatic operation. The technology for self-cohering of large arrays complements the imaging capability of conventional synthetic aperture radar (SAR) in two ways:

   a. It loosens the restriction associated with conventional SAR; specifically, it provides for:

      i. Variable, loose-tolerance flight paths by means of adaptive signal processing.

      ii. Reduced data rate through aperiodic data thinning.

      iii. Reduced effects of propagation anomolies through use of adaptive signal processing.

      iv. Improved RFI suppression through adaptive signal processing.

   b. It provides a real-aperture alternative to SAR for high-resolution imaging.

      i. No platform motion is required.

      ii. Arbitrary array configuration is permitted owing to individual-element phase control.

      iii. Tolerances are looser than conventional because of the adaptive signal processing.

      iv. Aperiodic or random thinning of large arrays provides greater frugality than conventional large filled arrays.

      v. Scanning is by sector (angle) as in conventional radar, rather than strip mapping as in conventional SAR.

Self-Cohering Techniques

A general self-survey technique for self-cohering of nonrigid antenna systems is described in [4]. That work has been extended to synthetic aperture systems and to near-field targets. The capability of the technique has been demonstrated with real synthetic-aperture radar data. The extended work is described in [5]. The purpose of the self-survey is to generate sufficiently accurate array element coordinates to permit beamforming and imaging. The self-survey is essentially a phase multilateration process. Phase measurements are made at each array element relative to either a cabled or broadcast reference. One set of self-survey equations applies to near-field bistatic receive-only arrays. These arrays can be real or synthetic. In the latter case the self-survey determines the sequence of positions of the moving receiver. A second set of self-survey equations applies to near-field monostatic transmit/receive arrays. Again, the arrays can be either real or synthetic. The monostatic and bistatic equations are sufficiently similar that essentially the same computer algorithm can be used for both cases. The first tests with monostatic synthetic aperture radar data produced element coordinates sufficiently accurate to permit nearly perfect imaging of isolated targets. Additional radar data is presently being analyzed.

Airborne Radio Camera

Following the doctoral dissertation on airborne distributed array concepts [6], we have proceeded to explore the requirements for an antenna element suitable for flush mounting in the aircraft skin. Professor Moshe Kisliuk from Tel-Aviv University is with us on sabbatical this year in order to do this work. He is extending the theory of the lossy transmission line to the microstrip-fed slot radiator above the ground plane. The theory is partially complete. Following its completion, an experiment will be conducted and a paper will be prepared for submission to the 1983 URSI Spring Meeting in Houston, Texas.

Imaging Experiments

Further progress has been made in two-dimensional, high resolution imaging using a cable array. This array consists of a single time-shared receiver moved along a 40 m cable that is hung between two towers 10 m high. The radar transmitter is a modified Air Force equipment (AN/APS-102). It radiates 60 nsec pulses 1,000 times/sec. The receiving equipment randomly selects 200-300 of the received echo traces as the receiver is moved across the cable. Our experiments have indicated essentially diffraction-limited performance from this nonrigid structure. This excellent performance results from our adaptive algorithm developed over the past few years. This work has been submitted to the Proceedings of the IEEE. Figures 1 - 3 compare images obtained by this equipment with optical photos of the same regions.

Based on our successful accomplishment last year in the use of the algorithm on airborne radar ground clutter [7], we sought to test our cable array system using targets of opportunity rather than an implanted corner reflector. The imaging results proved exceedingly satisfactory. This work will be reported in VFRC Quarterly Progress Report No. 42 [8].

Figures 1 and 2 compare 900 m x 240 mr maps of Phoenixville, PA, 5 km from the array. Adaptive beamforming was accomplished using a target of opportunity, a smokestack 8.2 km from the array (not shown in Figures 1 and 2). The radar map is a mosaic of twelve individual range-angle plots each 300 m in range by 60 mr in cross-range. The total picture contains 600 columns by 179 rows. The street map of Figure 2 was determined by measuring on the aerial photograph of Figure 1, then modifying to allow for non-parallelism of source-to-target radii for targets at different cross-range positions.

Figure 3 compares images of another target, the Cromby power plant some 8.2 km distant from the array. Part (a) is an optical telephoto (from the antenna site) of the radar-visible features of the plant (portion inside the delineated area); parts (b) and (c) are radar (range-angle) images of these features. A 1.2 m corner reflector was used for adaptive beamforming in (b), whereas a radar target of opportunity (the northernmost smokestock of the power plant indicated by arrows) was used in (c). Outlines of the power plant's major buildings and stacks have been added manually to parts (b) and (c) to indicate the relative positions of the radar-visible features.

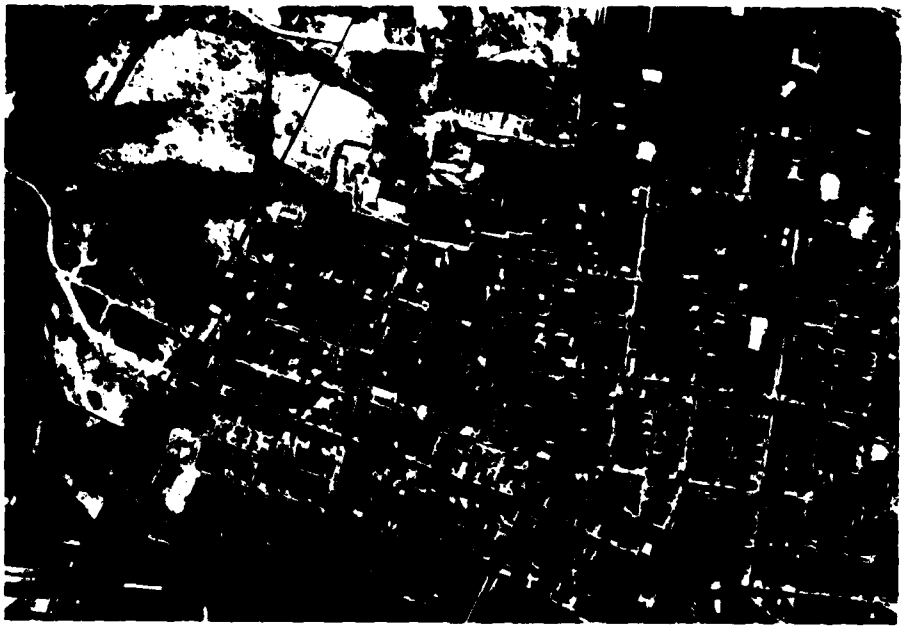

FIGURE 1. AERIAL PHOTO OF PORTIONS OF PHOENIXVILLE, PA.

FIGURE 2. RADAR MAP OF SAME AREA AS FIGURE 1.

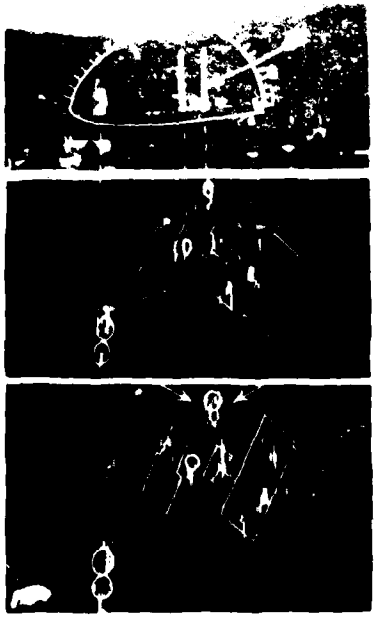

PART (a). OPTICAL TELEPHOTO FROM CENTER OF THE RADIO CAMERA ARRAY.

PART (b). RADAR IMAGE. BEAM-FORMER WAS A 1.2m CORNER REFLECTOR.

PART (c) RADAR IMAGE. BEAM-FORMER WAS A TARGET OF OPPORTUNITY. THE ARROWS HERE AND IN PART (a), ABOVE, IN-DICATE THE IMAGE AND PHOTO OF THE SMOKE-STACK TARGET USED AS BEAMFORMER.

FIGURE 1.3 OPTICAL AND RADAR IMAGES [illegible] POWER PLANT

Sidelobe Reduction by Interpolation

One of the major problems of large, thinned antenna arrays is the high sidelobe level that results from the thinning process and the resulting deterioration of microwave images. Several approaches to handling this sidelobe problem are being explored. The conventional beamforming algorithm, which is basically a Fourier procedure, assigns zero to all points of the radiation field that are not sampled (due to the thinning). While the Fourier technique is exceedingly robust, the imposition of zeros is a known error. We are studying procedures for interpolation of the radiation field as a better means of its representation at points where samples are not taken. Currently, we are exploring maximum entropy interpolation both on the field samples as well as on the autocorrelation estimates obtained from the field samples. To date, a few dB improvement on the peak sidelobe level has been achieved [9,10].

The use of diversity techniques is another approach to the reduction of the high sidelobes. Any technique which alters the details of the side radiation pattern without altering its statistics is helpful. Thus if the moduli of two radiation patterns having uncorrelated sidelobe patterns are averaged, the peaks tend to reduce toward the average sidelobe level and the valleys tend to fill in. *Element position diversity* is one such technique. Rearranging the locations of the elements of an array decorrelates the sidelobe pattern without changing its statistics.

A study has been completed on the efficacy of element position diversity in large, thinned random arrays, and a paper has been submitted on the subject. Asymptotic upper and lower-bound theories have been derived, and computer simulation shows that these bounds are very good. We have found that element position diversity is asymptotically efficient as the array grows large [11]. That is, averaging of two patterns reduces the peak sidelobe by nearly 2 dB.

The theory of the applicability of frequency diversity to the side radiation pattern also has been completed, and has been submitted to a journal. Both coherent (wideband waveforms) and noncoherent (frequency hopping) techniques have been studied. Asymptotic theories for high Q and low Q transmissions have been developed and have been found to check the simulated results exceedingly well [12]. The peak-to-average sidelobe level is approximately $\ln(L/\lambda)$ for high-Q waveforms and $\ln Q$ for low-Q waveforms.

A nulling technique for imaging with a sparse (high sidelobe) array was proposed and demonstrated in [13]. Theoretical development of that technique is in progress. It appears that the technique will permit imaging of targets with dynamic range greater than the mainbeam-to-average-sidelobe level of the array. It has been shown that the adaptive techniques (adaptive beamforming and self-survey) can be applied together with the nulling algorithm to obtain defraction-limited images despite sparseness of the elements and despite inaccuracies in element positions in a large array. The first report on this work will appear in the Valley Forge Research Center Quarterly Progress Report No. 42.

Image Feedback Control

The second major problem with large, thinned array systems is the uncertainty in element position that inherently occurs in such systems. While adaptive beamforming has proven exceedingly successful, it has been our goal for many years to develop techniques which were free of the dependence upon a reference radiating source. An important theorem by Muller and Buffington discovered nearly ten years ago indicates that it is possible to self-cohere a distorted aperture on the radiation field from an arbitrary scene, provided that the sources within the scene are spatially incoherent [14].

An examination of the optical image feedback process of Muller and Buffington has shown that it depends fundamentally on the non-coherent nature of light. Thus, the technique will not apply directly to coherent microwave radiation. In order for image feedback techniques to work with microwaves, some information regarding the nature of the target to be imaged is required. Such information can come from use of beacons, from range gating of target returns, etc. Thus the concept of image feedback is tied to the system design. This image feedback research will continue throughout the grant period.

REFERENCES

[1] C. N. Dorny, B. D. Steinberg, "High Angular Resolution Microwave Sensing with Large, Thin, Random Arrays", Annual Technical Report to Air Force Office of Scientific Research, UP-VFRC-16-79, Univ. of Pa. Nov. 1979.

[2] C. N. Dorny, B. D. Steinberg, Y. Bar-Ness, "High Angular Resolution Microwave Sensing with Large Thin, Random Arrays" Annual Technical Report to Air Force Office of Scientific Research, UP-VFRC-26-80, Univ. of Pa., Nov. 1980.

[3] C. N. Dorny and B. D. Steinberg, "High Angular Resolution Microwave Sensing With Large, Sparse, Random Arrays," Annual Technical Report to Air Force Office of Scientific Research, UP-VFRC-40-81, Univ. of Pa., Nov. 1981.

[4] Lee, Eu Anne, "A Generalized Self-Survey Technique for Self-cohering of a Large Array", Doctoral Dissertation in Electrical Engineering and Science, Univ. of Pa. Report UP-VFRC-30-81, August 1981.

[5] C. Nelson Dorny, Tianhu Lei, "Synthetic Aperture Near-field Self-survey", VFRC QPR No. 42, February, 1983.

[6] E. Yadin, "Phase Synchronizing Distributed, Adaptive Airborne Antenna Arrays", Univ. of Pa., Doctoral Dissertation, 1981.

[7] B. D. Steinberg, E. Yadin, "Radio Camera Experiment with Airborne Radar Data," Proceedings IEEE, Vol. 70, No. 1, January 1982.

[8] B. D. Steinberg, W. Whistler, D. Carlson, "Two-Dimensional Imaging with a Radio Camera", submitted to Proceedings IEEE with the Phoenixville photos.

[9] B. D. Steinberg, Harish M. Subbaram, "Image Quality Enhancement: Sidelobe Suppression by Interpolation", VFRC QPR No. 41, November 1982.

[10] Harish M. Subbaram, "Maximum Entropy Interpolation for Thinned Arrays," VFRC QPR No. 41, November 1982.

[11] B. D. Steinberg, E. Attia, "Sidelobe Reduction by Element Position Diversity", submitted to IEEE Trans. on Antennas and Prop., January 1982.

[12] B. D. Steinberg, E. Attia, "Raduction of Random Array Sidelobes by Frequency Diversity," submitted to the IEEE Trans. on Antennas and Prop., June 1982.

[13] B. D. Steinberg and D. J. Ho, "A Sidelobe Suppression Technique for the Radio Camera," VFRC QPR No. 29, May 1979.

[14] R. A. Muller and A. Buffington, "Realtime Decorrelation of Atmospherically Degraded Telescope Images Through Image Sharpening," JOSA 64, Sept. 1974, pp. 1200-1210.

PUBLICATIONS RESULTING FROM AFOSR SUPPORT

Yeheskel Bar-Ness and A. Heiman, "Optical Design of a PLL with Two Separate Phase Detectors," IEEE Trans. Communications, February, 1981, pp. 92-100.

Bernard D. Steinberg and Ajay K. Luthra, "Asymmetries in the Diffraction Pattern of an Asymmetrical Aperture," IEEE Trans. Antennas and Propagation, July 1981.

Bernard D. Steinberg, "Radar Imaging with a Distorted Array: The Radio Camera Algorithm and Experiments," IEEE Trans. Antennas and Propagation, Vol. AP-29, No. 5, Sept. 1981, pp. 740-748.

Yeheskel Bar-Ness and Hagit Messer, "Wideband Instantaneous Frequency Measurements (IFM) Using SAW Devices," IEEE Trans. Sonics and Ultrasonics, Nov. 1981.

*Bernard D. Steinberg and Eli Yadin, "Radio Camera Experiment with Airborne Radar Data," Proc. IEEE, Vol. 70, No. 2, January 1982.

*Bernard D. Steinberg and Eli Jadlovker, "Distributed Airborne Array Concepts," IEEE Trans. Aerospace and Electronic Systems, Vol. EAS-18, No. 2, March 1982.

Eu Anne Lee and C. Nelson Dorny, "A Generalized Self Survey Technique for Self Cohering Large Arrays," submitted to IEEE Trans. Antennas and Propagation, May 1982.

*Bernard D. Steinberg, "Properties of Phase Synchronizing Sources for a Radio Camera," IEEE Trans. Antennas and Propagation, November 1982, pp. 1080-1092.

*Bernard D. Steinberg, "Phase Synchronizing a Nonrigid, Distributed, Transmit-Receive Radar Antenna Array," IEEE Trans. Aerospace and Electronic Systems, September 1982, pp. 609-620.

IN PREPARATION FOR PUBLICATION

Chung H. Lu and C. Nelson Dorny, "Interference Cancellation in Self-Cohering Arrays," to be submitted to IEEE Trans. on Antennas and Propagation.

Chung H. Lu and C. Nelson Dorny, "Ambiguity Resolution in Self-Cohering Arrays," to be submitted to IEEE Trans. on Antennas and Propagation.

*Attached

INTERACTIONS

B. D. Steinberg, W. Whistler, D. Carlson and E. Yadin-Jadlovker, "Two recent radio camera experiments," Benjamin Franklin 1982 Symposium on Advances in Antenna and Microwave Technology, 15 May 1982.

E. H. Attia, "Sidelobe reduction of random arrays by element position diversity," University College, London, June 14, 1982.

E. H. Attia, "The Giant Radio Camera project at VFRC," University College, London, June 16, 1982.

PROFESSIONAL PERSONNEL

Professors C. Nelson Dorny, Bernard D. Steinberg, Raymond S. Berkowitz

Graduate Students: Hashem Attia, Lih-tyng Hwang, S. T. Juang, Tianhu Lei, Jenho Tsao, Geoffrey Edelson

Research Specialists: Earl N. Powers, William Whistler

Visiting Scholars: Yun Long Zhang, Hong Yuan Chen

APPENDIX

Papers published in 1982

Properties of Phase Synchronizing Sources for a Radio Camera

BERNARD D. STEINBERG, FELLOW, IEEE

Abstract—A distorted phased array can be made to operate as a diffraction-limited aperture if a compensating time delay and/or phase shift is added in each antenna element channel. When the distortion is not known *a priori* the correction must be based upon phasefront measurements of the radiation from a source external to the array. The ideal adaptive synchronizing source is a point source radiating in free space. The phasefronts of realistic sources are perturbed, however. Three types of practical sources and calculations of the conditions under which their radiation fields are acceptable for adaptive beamforming are discussed. The sources are the passive reflector, the active beacon, and radar ground clutter.

I. INTRODUCTION

A RETRODIRECTIVE array samples the radiation field from a point source at a distance and adjusts the phase of the radiated wave at each element to be the complement of the measured signal phase [1]–[3]. The radio camera (distorted array plus self-adaptive beamforming) requires retrodirective procedures [4]–[8]. The function of the radio camera is very high angular resolution imaging. The aperture size required at microwaves to achieve the resolving power of common optical instruments, which is 10^{-5} to 10^{-4} rad, is hundreds of meters to tens of kilometers, as is evident from the relation $\Delta\theta \simeq \lambda/L$, where $\Delta\theta$ is the beamwidth, λ is the wavelength, and L is the size of the aperture. Apertures so large will be very *difficult if not impossible to survey* to the one-tenth wavelength or smaller tolerance required for diffraction-limited operation [5]. Some apertures will flex and may even be time-varying. Earlier papers describe various aspects of the radio camera. The overall system concept is given in [4] and [5]. The details of the algorithm for searching for the retrodirective beamformer, focusing upon it, and scanning the focused beam in range and angle are given in [7]. Early experimental results were published in that paper and in [6] and [8].

This paper examines the retrodirective beamforming source and determines the required properties for satisfactory operation of a radio camera. The principle of operation with a distorted array, the radiation pattern that results from retrodirective beamforming, and the losses that can develop in array gain are discussed in the next two sections. In the following section bounds are calculated on the necessary physical properties of retrodirective synchronizing sources. The sources discussed include the passive reflector such as the corner reflector, the active beacon and radar ground clutter. Experimental one-dimensional radio camera images show how array gain can be degraded by an imperfect retrodirective source.

Manuscript received June 30, 1981; revised October 16, 1981. This work was principally supported by the Office of Naval Research and the Air Force Office of Scientific Research.

The author is with the Valley Forge Research Center, Moore School of Electrical Engineering, University of Pennsylvania, Philadelphia, PA 19104 and the Airborne Radar Branch, Naval Research Laboratory, Washington, DC 20375.

THE RADIO CAMERA

Fig. 1 shows a pulsed transmitter illuminating a point reflector which reradiates to a distorted receiving array. The array system measures time and/or phase differences between the echoes at each antenna element and assumes that they are due entirely to differential distances from the source to the antenna elements and to variations in the index of refraction of the propagation medium along the ray paths. Following envelope time-delay correction, an automatic phase correction $\phi_0 - \phi_n$ is made, which is the difference between the echo phases received at some arbitrary reference element and the nth element. The second term $-\phi_n$ is the key to the corrective process. It is the complement of the phase of the received signal relative to some reference phase which is constant across the array. In practice, the reference signal need not be the signal from another element in the array; instead, it can be the local oscillator wave from a central source in the system delivered to each element with the same phase. Either procedure is satisfactory.

Automatic phase conjugation also is called adaptive beamforming or self-cohering or phase synchronizing. After the beam is formed it may be scanned by geometrically calculated phase corrections applied open loop to the second bank of phase shifters. Analog or digital circuits can be used to implement both banks of phase shifters and the phase controllers.

The result of adaptive beamforming is a receiving array self-focused upon the synchronizing source. The dimensions of the focal zone of the array when focused upon a near-field source at a distance R are shown in Fig. 1. The nominal cross-range beamwidth is $\lambda R/L$. The beamwidth in range is the depth of field of the aperture, which is approximately $7\lambda(R/L)^2$ [5]. The focal zone when the source is in the far field is an angular sector of width λ/L rad. Thus, the angular resolution in the scanned image of the radio camera is essentially the same in the near field as in the far field. The far-field range resolution is determined by the pulse duration of the transmitter (expressed in distance units) and in the near field it is the pulse duration or the depth of field, whichever is smaller.

Fig. 2 shows two one-dimensional radio camera images which illustrate the importance of a high quality beamforming source. These one-dimensional angle scans were obtained with a modified AN/APQ-102 radar operating in the synthetic aperture radio camera mode described in [6], [7], and [9]. The array was approximately linear. Its length was 40 m. It consisted of 200 sample points located at random. The radar was an X-band (λ = 3 cm) set with 50 kw peak power and a range cell of 9 m. The adaptive beam-forming source in the experiment of Fig. 2(a) was a 4 ft corner reflector 5.6 km from the radar. 31 m more distant was a 2 ft corner reflector. The radio camera first self-focused upon the 4 ft reflector, then scanned in angle and range to the location of the smaller reflector, following which it scanned in angle across it to produce the image shown in Fig. 2(a). The ordinate is in ampli-

0018-926X/82/1100-1086$00.75

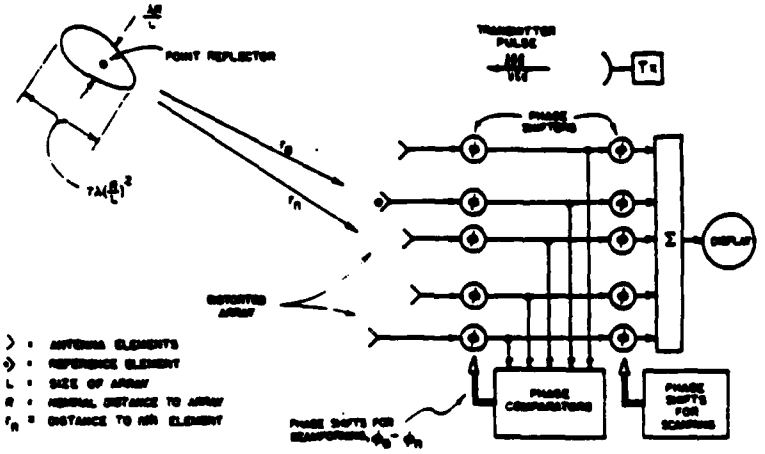

Fig. 1. Phase synchronizing a badly distorted radio camera array on echoes from a point reflector.

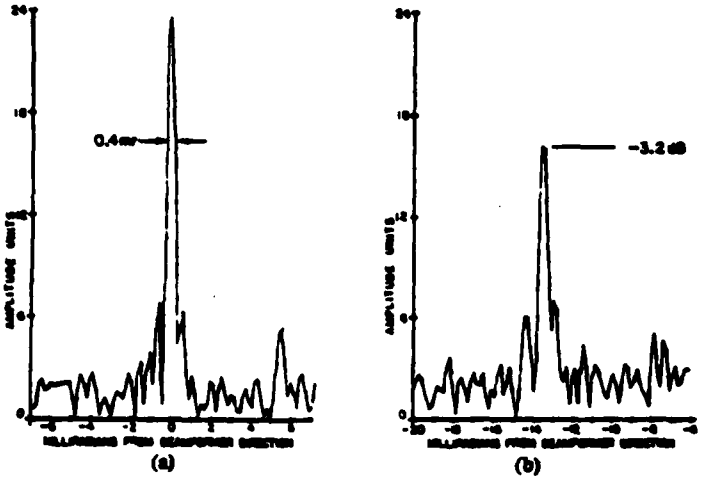

Fig. 2. One-dimensional radio camera images of a two-ft corner reflector at 5.6 km. Beamforming target in (a) is another corner reflector; in (b) it is a house. Loss in array gain is 3.2 dB.

tude units, and the abscissa is in milliradians from the direction to the 4 ft reflector. The cross section of the imaged 2 ft reflector is 0.4 mrad which is 2.2 m at the target range. The expected values based upon diffraction theory, synthetic array theory, and random array theory are the same.

Fig. 2(b) shows the same target imaged by the same equipment using exactly the same array and imaging algorithm. The only difference is the beamforming source. The source in Fig. 2(b) is a house located 15.5 mrad to the left of the target and 45 m from it in range. The resolving power of the instrument is not significantly altered but the array gain is reduced by 3.2 dB.

That the array gain is seriously affected by the properties of the synchronizing source, while the array beamwidth is not, is predictable from random array theory [5]. Array gain is sensitive to random phase errors across the array according to $E\{G/G_0\} = \exp[-\sigma_\phi^2]$ where $E\{\cdot\}$ means expectation, G is the array power gain, G_0 is the gain in the absence of errors, and σ_ϕ^2 is the phase-error variance across the array. Expressed in decibels the loss in gain is $\Delta G(\text{dB}) = 4.3\ \sigma_\phi^2$. Based on these equations it may be deduced that the phase variance across the array after phase synchronization on the echoes from the house was 0.74 rad^2 or 0.86 rad rms. The nominal widths of all lobes (main lobe and sidelobes) of a random array remain unchanged irrespective of the phase errors. Thus, phase errors during the adaptive beamforming process reduce array gain but have no first-order effect upon array beamwidth.

It is evident that the house was not a satisfactory target of opportunity for adaptive phase synchronization of the distorted array. In the following sections the conditions under which targets are satisfactory sources are examined and bounds are derived for their use.

LOSS IN ARRAY GAIN

The radiation power pattern formed by the adaptive retrodirective process is approximately a replica of the source function or scene that produces the incident radiation field. Let the source or scene be at distance R from the distorted array (Fig. 3). Let y be an axis through the scene perpendicular to the direction of phase synchronization of the array, which will be called the z-axis. Define the reduced angular variable $u = \sin\theta = y/R$ where the angle θ is measured from the z-axis. θ is called the scan angle. The source or scene $s(u)$ produces a radiation field along the x-axis in the array (Fresnel approxi-

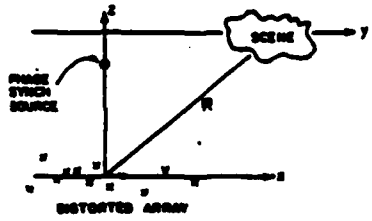

Fig. 3. The scene to be imaged is at distance R from the array. The z-axis is in the direction of the synchronizing source. The x- and y-axes are perpendicular to the z-axis and are in the same plane.

mation)

$$S(x;R) = \int s(u) e^{jk(xu - x^2/2R)}\, du \tag{1}$$

where the x-axis also is perpendicular to the z-axis. Now assume a phase conjugation operation such that the current excitation in the array along the x-axis is the complex conjugate $S^*(x)$ of (1). The radiation pattern of the array in the source region becomes

$$f(u;R) = \int S^*(x;R) e^{jk(xu - x^2/2R)}\, dx \tag{2}$$

which implies

$$S^*(x;R) e^{-jkx^2/2R} = \int f(u;R) e^{-jkxu}\, du \tag{3}$$

by the properties of the Fourier transform. Equation (3) may be rewritten

$$S(x;R) = e^{-jkx^2/2R} \int f^*(u;R) e^{jkxu}\, du \tag{4}$$

from which, by comparison with (1), it is evident that the radiation pattern $f = s^*$ or $|f| = |s|$, thus validating the opening statement of this section. Now introduce a discrete sampling of the radiation field in the x-axis at locations x_l and let the adaptive circuits weight the N elements by $w_l = S^*(x_l;R)$. The radiation pattern

$$f_a(u;R) = \int_L \sum_{l=1}^{N} S^*(x_l;R) \delta(x - x_l) e^{jk(xu - x^2/2R)}\, dx \tag{5}$$

is an approximation to (2), the approximation being due to the discrete sampling in the aperture and to its finite extent L. In (5) $\delta(\cdot)$ is the Dirac-delta function. Since the array is not likely in the x-axis (5) is not an exact expression of the radiation pattern but is a close approximation in the angular neighborhood of the adaptive beamforming source.

A further approximation is made in the radio camera: since the amplitude of the radiation field must be nearly constant over the source to approximate a point source, it is sufficient merely to phase-weight the elements in the array by the conjugate of the incident field and to ignore its amplitude variation.

Based on this reasoning, it is seen that when various scattering centers exist in the source region the gain of the adaptively formed beam will be reduced from its maximum possible value due to the gain of the radiation pattern in the directions of those scatterers. The scatterers may be part of the synchronizing target, as in the case of the house (Fig. 2(b)), or they may be clutter scatterers in the patch illuminated by the transmitter. To calculate the loss in gain it is necessary only to relate the phasefront distribution to the scatterer distribution and then deduce the gain loss from the phase-front distortion.

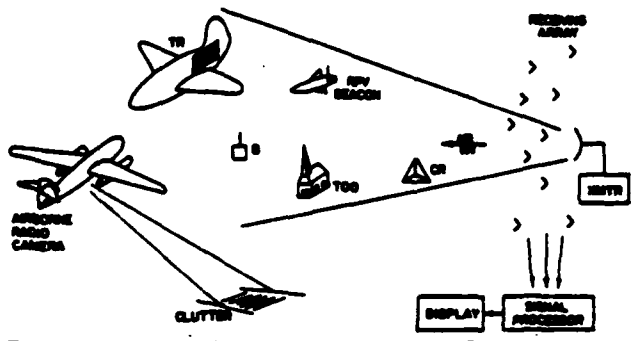

Fig. 4. Types of synchronizing sources: passive reflectors, active beacons, and distributed clutter.

First, the scatterer distribution, whether on the beamforming target or in the illuminated clutter patch, may be presumed to be random, which is a sufficient condition to ensure that the phase perturbations in the phasefront of the reradiation also are random. Given this condition the loss in gain, in decibels, is 4.3 σ_ϕ^2. Next, assume that a tolerable loss in gain is 1 dB. The phase variance allowed in the phasefront is $\sigma_\phi^2 = 1/4.3$ rad^2. Now assume that the target having radar cross section σ_T radiates as a point source and that the clutter cross section $\sigma_C < \sigma_T$. Their echoes received at some arbitrary antenna element in the array arrive with abritrary phase α and amplitude ratio $a = \sigma_C^{1/2}/\sigma_T^{1/2} < 1$. The phase error $\delta\phi = \tan^{-1}[a \sin \alpha/(1 + a \cos \alpha)]$ is a zero mean random variable. Equating its variance to 1/4.3 leads to the condition $\sigma_T \geq 2.5\, \sigma_C$, which guarantees that the loss in gain will not exceed tolerance.

TYPES OF SYNCHRONIZING SOURCES

Fig. 4 illustrates several types of synchronizing sources. Shown on the ground are a corner reflector (CR), which is a near-ideal beamforming source, and a large, prominent target of opportunity (TOO). Both are passive reflectors. Also shown is an active beacon (B). The beacon can be airborne as well, as illustrated by the one carried in the remotely piloted vehicle (RPV). The beamforming target also may be a reflecting surface on the target to be imaged (called a target reference (TR)), as is illustrated by the large specular reflecting surface of the airplane target. Lastly, the beamforming source can be distributed clutter echoes as is illustrated for the airborne radio camera. These three types of sources (passive reflector, active beacon and distributed clutter) are discussed separately in the subsections below.

Passive Reflector

Not only must the passive reflector have a large enough radar cross section so that its echo dominates the phasefront of the radiation field illuminating the array, but its physical size must be small enough so that its reradiation is nearly planar or spherical. These two conditions place bounds on the acceptable size of a passive target.

The nominal lobe spacing of the radiation from a target of size T is λ/T. That this is so may be seen by considering structures of simple or known characteristics. For example, a flat-plate reflector of length T radiates a pattern having the angu-

lar characteristic $\sin(\pi Tu/\lambda)/(\pi Tu/\lambda)$, where $u = \sin(\theta - \theta_0)$, θ is the angle measured from the normal to the surface, and θ_0 is the direction of maximum reradiation. The width of the main lobe is approximately λ/T, as is the spacing between zero crossings in the remainder of the reradiation pattern. Similarly, if the target contains two prominent scatterers of equal strength spaced by T the reradiation pattern has the form $\cos(\pi Tu/\lambda)$. The zero-crossing interval is λ/T. If the scatterers are of unequal strength the radiation pattern develops an additive constant but the angular modulation period remains the same. Lastly, if a target consists of many scatterers of random amplitudes and locations within the interval T the results will be similar. Let the scatterer distribution be a sample function of a random process characterized by $\sum a_l \delta(y - y_l)$, where a_l are the scattering amplitudes and y_l are their locations on the reflector. The radiation pattern is

$$g(u) = \int_{-\frac{T}{2}}^{\frac{T}{2}} \sum a_l \delta(y - y_l) e^{jkyu}\, dy$$

$$= \frac{\sin(\pi Tu/\lambda)}{\pi Tu/\lambda} * \sum a_l e^{jky_l u} \tag{6}$$

where the asterisk means convolution. The second term is the underlying radiation pattern of the collection of scatterers. The first term is due to the truncation of one random process; it is the Fourier transform of the window function representing the extent of the target. The lobe spacing of $g(u)$ can be no smaller than that of the sync function, which is λ/T. All three examples indicate λ/T to be a typical value of the lobe spacing. A lobe width is about half this value, and its cross section at the array a distance R from the target is $\lambda R/2T$. Unless the central portion of such a lobe encompasses the entire array the second condition above is not satisfied. Hence, a minimum condition for satisfactory beamforming is

$$\frac{\lambda R}{2T} > L \text{ or } T < \frac{\lambda R}{2L}. \tag{7}$$

To satisfy the first condition the radar cross section of the adaptive beamformer must exceed the combined cross sections of all the scatterers in the illuminated patch so as to dominate the phasefront. The clutter cross section $\sigma_C = A_C \sigma_0$, where $A_C = R\Delta R\Delta\theta$ is the area of the patch illuminated by the transmitter, $\Delta\theta$ is the nominal beamwidth, ΔR is the pulse length, and R is the distance from the transmitter. σ_0 is the normalized backscatter coefficient of the terrain. The radar cross section of the target $\sigma_T = A_T G$, where A_T is the projected target area illuminated by the transmitter, and G is the gain or directivity of the target reradiation in the direction of the receiver. The peak gain of a flat plate reflector is $4\pi A_T/\lambda^2$ and its maximum radar cross section is $\sigma_T = 4\pi A_T^2/\lambda^2$ which equals $4\pi T^4/\lambda^2$ for a square reflector of side T. Since the effective area of a corner reflector is that of the inscribed equilateral hexagon, its area is $T^2/2\sqrt{3}$ and its radar cross section is approximately T^4/λ^2. Radar cross sections of other standard shapes are well documented [10].

By using the condition $\sigma_T \geq 2.5\,\sigma_C$ derived earlier, and expressing σ_T and σ_C in terms of radar and target parameters, the lower bound on target size is easily calculated for any shape. For example, by using the last expression above for target cross section the inequality $T^4/\lambda^2 < 2.5\,\sigma_0 R\Delta R\Delta\theta$ expresses a lower bound upon corner reflector target size. Combining it with (7) yields

$$(2.5\lambda^2\sigma_0 R\Delta R\Delta\theta)^{1/4} < T < \frac{\lambda R}{2L}. \tag{8}$$

TABLE I
MAXIMUM AND MINIMUM SIZES OF CORNER REFLECTORS FOR USE AS SOURCES FOR X-BAND AND L-BAND ILLUSTRATIONS

Band	λ (m)	σ_0	ΔR (m)	$\Delta\theta$ (rad)	λ/L	T_{min} (m)	T_{max} (m)
X	0.03	10^{-2}	5	1/20	1/2000	0.25	5
L	0.3	10^{-3}	20	1/20	1/2000	0.61	5

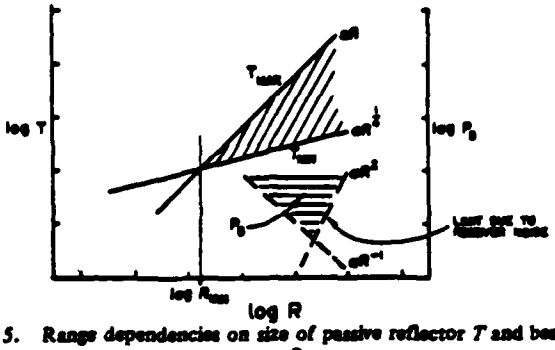

Fig. 5. Range dependencies on size of passive reflector T and beacon power P_B.

Table I illustrates two cases of radars with beamwidths of 1/20 rad or approximately 3°. One has a 3 cm wavelength and a 5 m range resolution. The other has a 30 cm wavelength and a 20 m range resolution. In each case the design problem is to make the azimuthal resolution 100 times finer through the use of a large, distributed, receiving phased array. The adaptive beamformer is at a distance of 10 km in both cases. Values of $\sigma_0 = 10^{-2}$ and 10^{-3} are assumed for the two wavelengths. The right side of the table shows the maximum and minimum sizes of corner reflectors that satisfy the requirements described above.

Fig. 5 expresses the bounds as a function of range R. It is evident that at short ranges the minimum allowed size exceeds the maximum allowed size, which means that adaptive beamforming cannot be accomplished with a passive reflector at distances less than some minimum range. The minimum range is found by equating the bounds:

$$R_{min} = (40L^4\lambda^{-2}\sigma_0\Delta R\Delta\theta)^{1/3}. \tag{9}$$

Active Beacon

The second phase synchronizing source is an active beacon triggered by the radar transmitter radiating a pulse sequence of power P_B at a distance R from the array. Isotropic radiation is assumed. The beacon power density at the array is $P_B/4\pi R^2$. The clutter power density at the array is $P_T G_T \sigma_C/(4\pi R^2)^2$ where P_T is the radar transmitter power and G_T is the antenna gain [11]. The clutter cross section σ_C was given in the subsection above. Combining these terms and requiring that the beacon signal exceed the clutter echo by a factor of 2.5 or more results in the following condition on the beacon power:

$$P_B \geq \frac{P_T G_T \sigma_0 \Delta R\Delta\theta}{1.6\pi R}. \tag{10}$$

Whereas the required size of the passive target grows with range (see (8)), the minimum required beacon power is inversely proportional to distance. This surprising result is due to the fact that the beacon power density at the receiver suffers an inverse square propagation loss while the clutter power decreases with the cube of range. P_B cannot decrease indefinitely with range because the beacon signal always must exceed receiver noise. Based on the assumption that receiver noise is independent from antenna-element channel to channel the received signal must exceed the noise by the same factor of 2.5 as it must exceed the clutter. The received beacon signal power is $P_B A_R/4\pi R^2$, where A_R is the effective area of the entire receiving array. Receiver noise power is $kTBF$ where k is Boltzmann's constant, T is receiver temperature, B is receiver bandwidth, and F is the system noise figure. Combining these expressions leads to the second requirement upon beacon power:

$$P_B > \frac{10\pi R^2 kTBF}{A_R}. \tag{11}$$

These equations also are plotted in Fig. 5. If the beacon is self-triggered (radar transmitter turned off) the weak demand upon beacon power given by (10) vanishes.

Due to the different range dependencies of the passive target and the active beacon, the following general observations may be made:

- A TOO, which is required for synchronizing a mobile radio camera, is most likely to be found at a short distance from the radar.
- A fixed installation can use an implanted source. The choice of active beacon triggered by the radar transmitter versus passive reflector will be influenced by the distance from source to radar (short range favors a passive source and long range favors the beacon).

Clutter as a Synchronizing Source

Earlier it was shown that the beam pattern, following self-cohering, approximates the source function that produces the incident radiation field. If the echoes are primarily from clutter the pattern will approximate the angular clutter distribution weighted by the pattern of the illuminating beam. Its width, therefore, will be the same as that of the transmitter, and no resolution improvement will result. When the radar system is airborne, however, echoes from scatterers within the ground patch may be distinguished from each other by their Doppler shifts; hence, narrow-band filtering of the received clutter echoes can extract the reflections from scatterers within a subpatch of the desired width. The output of such a filter can be used as a phase-synchronizing reference [5].

Fig. 6 shows an airborne radar moving with speed V illuminating a clutter patch with beamwidth $\Delta\theta$ at distance R and at angle θ from the ground track. The receiving array of length L is assumed to be distributed on the airframe. The width of the clutter patch $R\Delta\theta = R\lambda/a$, $a \ll L$ is the aperture of the radar transmitter, whereas the proper width cannot exceed $\lambda R/2L$, as derived in (7). Assuming that the aircraft altitude is much smaller than the range, the Doppler shift of an echo from a scatterer at angle θ is

$$f_d = 2V \cos\theta/\lambda. \tag{12}$$

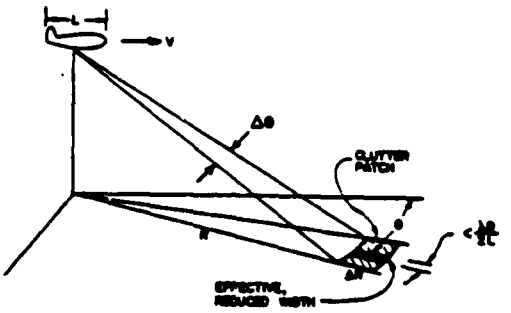

Fig. 6. The clutter patch is too wide to be a synchronizing source. Narrow-band filtering in the receiver reduces effective patch width to $\lambda R/2L$.

To confine the response of the filter to echoes from the desired subpatch its bandwidth

$$W < \frac{2V}{\lambda}\left[\cos\left(\theta - \frac{\lambda}{4L}\right) - \cos\left(\theta + \frac{\lambda}{4L}\right)\right]$$

$$= \frac{4V}{\lambda}\sin\frac{\lambda}{4L}\sin\theta \simeq \frac{V}{L}\sin\theta. \tag{13}$$

Fig. 7 shows how the reference signal would be used.[1] One element is chosen as the reference element. A narrow-band filter (NBF) of bandwidth W centered at the mean Doppler shift delivers the reference signal to a bank of phase detectors, each associated with one antenna element. The clutter echoes received at each antenna element pass through a voltage-controlled phase shifter to the summer of the phased array. The signal also passes to the other input of the phase detector. The beat product is smoothed in a low pass filter and applied as the control voltage to the phase shifter. The circuit is a phaselock loop which drives the two inputs to the phase detector into a quadrature relationship. The loop responds to those components of the element signal which correlate with the narrow-band reference signal.

Fig. 8 shows the clutter spectrum at an arbitrary element and after passage through the NBF. The clutter signal may be represented by the sum of M sinusoidal echoes of amplitudes a_l, Doppler shifts $f_d + f_l$ where $f_d = 2V\cos\theta/\lambda$ is the mean shift, and phases ϕ_l. The a_l, f_l and ϕ_l are independent random variables. In addition, there is a phase shift Φ due to the position of the element in the distorted array; Φ is the quantity to be corrected by the adaptive process. Calling the clutter signal $c(t)$, its equation is

$$c(t) = \sum^{M} a_l \cos\left[(\omega_0 + \omega_d + \omega_l)t + \phi_l + \Phi\right] \tag{14}$$

where $\omega = 2\pi f$. The reference wave is the sum of $K < M$ echoes from the central portion of the ground patch. Its waveform is

$$r(t) = \sum^{K} a_l \cos\left[(\omega_0 + \omega_d + \omega_l)t + \phi_l\right]. \tag{15}$$

[1] A receiver chain containing the usual circuits such as amplifiers, mixer, and local oscillator is implicit in each channel. Coherent detection also is implicit. The NBF is assumed to be preceded by a range gate so that the NBF responds only to scatterers in the range interval $[R, R + \Delta R]$. Similarly, a range gate is assumed at the signal-input port of the phase detector. The analysis which follows also pertains to wide-band delay-line filters having narrow passbands at intervals of the pulse repetition frequency and to optical correlators [11].

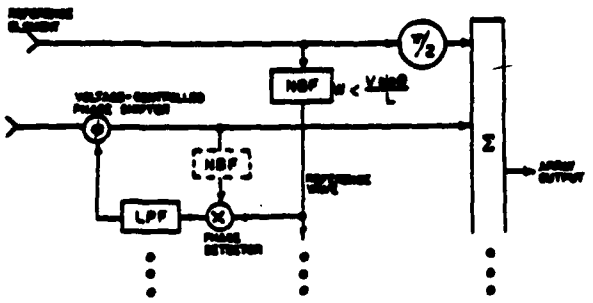

Fig. 7. Reference element and one other element in airborne radio camera. All signals phaselocked by clutter-derived reference wave obtained from narrow-band filter.

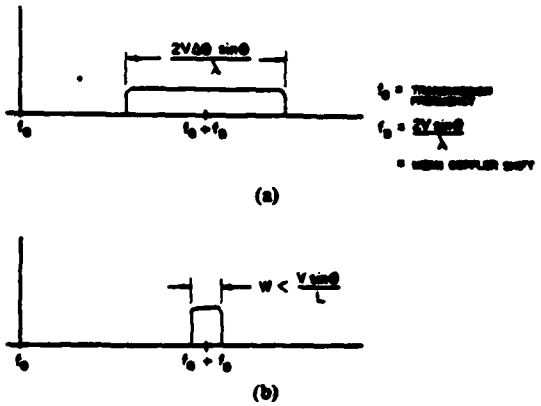

Fig. 8. (a) Input clutter spectrum. (b) After narrow-band filter in reference channel.

The mixer output is the product $e(t) = c(t)r(t)$, only the low frequency terms of which pass through the low pass filter. Its output voltage is

$$v(t) = \frac{1}{2} \sum_{l}^{M>K} \sum_{j} a_l a_j \cos[(\omega_l - \omega_j)t + \phi_l - \phi_j + \Phi]$$

$$= \frac{1}{2} \cos \Phi \sum^{K} a_j^2 + \frac{1}{2} \sum_{l \neq j}^{M>K} \sum a_l a_j \cdot \cos[(\omega_l - \omega_j)t + \phi_l - \phi_j + \Phi]. \quad (16)$$

The dc output is $\overline{v(t)} = K\overline{a^2} (\cos \Phi)/2$ where $\overline{a^2}$ is the mean square echo strength of the scatterers. Thus, the dc control voltage for the phase shifter is proportional to $\cos \Phi$. Since the loop drives this voltage to zero, the portion of the phase-shifted element signal within the passband of the NBF is brought into phase quadrature with the reference signal independent of the array distortion-induced phase error Φ. This procedure is performed in all array-element channels, resulting in the cophasing of their signals. The reference signal channel may be added provided that it is shifted in phase by $\pi/2$. The sum is the array output. Adding the NBF (shown dashed) in the PLL improves both its acquisition and tracking characteristics by reducing the phase noise in the loop. The steady state phase-error variance in the loop is proportional to the variance of (16) which is the power in the second term. That term consists of $K(M-1)$ sinusoids of average amplitude $1/2\overline{a_l a_j} = 1/2\overline{a_l}\,\overline{a_j} = 1/2\overline{a^2}$, assuming that the scatterers are statistically independent and have common statistics. Since the Doppler shifts and scatterer phases are independent from scatterer to scatterer the average power in the second term is the sum of the component powers, each of which contributes $1/2(1/2\overline{a^2})^2 = \overline{a^4}/8$. Hence, the variance of (16) is $\sigma_v^2 = K(M-1)\overline{a^4}/8$.

By adding the dashed NBF's in the element channels the number of scatterers in the clutter signal (13) drops from M to K, which reduces the variance to $\sigma_{v,NB}^2 = K(K-1)\overline{a^4}/8$. The reduction in phase-noise power is the factor $(M-1)/(K-1) \simeq M/K$ since the number of scatterers is large. This ratio is $2L\Delta\theta/\lambda$, which is approximately the ratio of the clutter bandwidth to the filter bandwidth because random ground and sea clutter typically exhibit uniform angular distributions and the transformation (12) from angle to frequency shift is, for small angles, nearly constant. This phase-noise power reduction factor is exactly the angular resolution improvement ratio, which can be very large. For example, consider an S-band radar ($\lambda = 10$ cm) with a 3° beamwidth ($\Delta\theta \simeq 1/20$ rad) aboard a 30 m aircraft. The resolution improvement factor is 30, which means that the reduction in the phase-noise power in the PLL can be as large as 15 dB when the NBF is added in the loop.

In addition to the proper filter bandwidth (13) the frequency selectivity of the filter must ensure that the clutter power of the echoes passing through the central region of the filter exceeds the remainder by at least a factor of 2.5, or 4 dB. Let the clutter power density spectrum be represented by $C(f)$ and the filter transfer function by $H(f)$, where the origin of the frequency variable f is taken at the mean Doppler shift f_d. Based on (12) and the assumption above of a uniform angular distribution of scatterers, $C(f)$ is proportional to the probability density function of the frequency variable in (12) and the weighting due to the antenna pattern. The former can be shown to be proportional to $[(2V/\lambda)^2 - f^2]^{-1/2}$. The latter is the two-way antenna pattern transformed from the angle variable θ to the frequency variable f using (12). The required condition on $H(f)$ is given by

$$\frac{\int_0^{W/2} C(f)|H(f)|^2\,df}{\int_{\frac{W}{2}}^{\infty} C(f)|H(f)|^2\,df} \geq 2.5. \quad (17)$$

SUMMARY

A distorted phased array can be made to operate as a diffraction-limited aperture if a compensating phase shift is added in each antenna element channel. When the distortion is not known *a priori* the phase correction must be based upon phasefront measurements of the radiation from a source external to the array. The ideal phase synchronizing source is a point source radiating in free space. The phasefronts of realistic sources are perturbed, however. This paper discusses three types of practical sources and calculates the conditions under which their radiation fields are acceptable for adaptive beamforming.

The most important source is a passive reflector such as a corner reflector or a large target of opportunity. It is shown

that bounds exist on the minimum and maximum sizes of such reflectors and that there is some minimum distance below which the conditions cannot be met. The bounds on size T when the synchronizing source is a corner reflector and the minimum range R_{min} are

$$(2.5\lambda^2\sigma_0 R\Delta R\Delta\theta)^{1/4} < T < \frac{\lambda R}{2L} \tag{8}$$

$$R_{min} = (40L^4\lambda^{-2}\sigma_0\Delta R\Delta\theta)^{1/3}. \tag{9}$$

An active beacon is an excellent adaptive beamforming source. The required beacon power decreases with range according to the relation

$$P_B \geq \frac{P_T G_T \sigma_0 \Delta R\Delta\theta}{1.6\pi R} \tag{10}$$

until such a range is reached at which receiver noise competes with the beacon signal. Beyond that range the beacon power must increase with distance according to

$$P_B \geq \frac{10\pi R^2 kTBF}{A_R}. \tag{11}$$

It is also possible to use clutter echoes to phase synchronize a distorted array provided that the radiation from scatterers located at different angular positions in the ground patch can be distinguished in the receiver. This condition can be met if the radar is on a moving platform, for then the scatterer echoes are Doppler shifted in proportion to $\cos\theta$. Narrow-band filters in each antenna element channel respond only to echoes from scatterers in a narrow angular or cross-range swath no larger than T_{max} given above. The procedure permits the extraction from the clutter echoes of a reference signal to phase synchronize the array, thereby permitting the technique to be applied to an airborne distributed antenna array aboard a nonrigid aircraft. The first condition on the filter bandwidth is

$$W \leq \frac{V\sin\theta}{L} \tag{13}$$

and on the frequency selectivity of its transfer function $H(f)$ it is

$$\int_0^{W/2} C(f)|H(f)|^2\,df \geq 2.5\int_{W/2}^{\infty} C(f)|H(f)|^2\,df. \tag{17}$$

$C(f)$ in (17) is the clutter power density spectrum.

REFERENCES

[1] *IEEE Trans. Antennas Propagat.*, vol. AP-12, no. 2, Mar. 1964, Special Issue on Active and Adaptive Antennas (contains 13 papers on retrodirectivity).

[2] R. C. Hansen, Ed., *Microwave Scanning Antennas*, vol. 3, New York: Academic, 1964. (See ch. 5 by D. L. Margerum.)

[3] R. C. Chernoff, "Large active retrodirective arrays for space applications," *IEEE Trans. Antennas Propagat.*, vol. AP-27, no. 4, pp. 489–495, July 1979.

[4] B. D. Steinberg, "Design approach for a high-resolution microwave imaging radio camera," *J. Franklin Inst.*, vol. 296, no. 6, pp. 415–432, Dec. 1973.

[5] ——, *Principles of Aperture and Array System Design*. New York: Wiley, 1976.

[6] B. D. Steinberg, E. N. Powers, D. Carlson, B. Meagher, Jr., R. S. Berkowitz, C. N. Dorny, and S. H. Seeleman, "First experimental results from the Valley Forge radio camera program," *Proc. IEEE* pp. 1370–1371, Sept. 1979.

[7] B. D. Steinberg, "Radar imaging from a distorted array: The radio camera algorithm and experiments," *IEEE Trans. Antennas Propagat.*, pp. 740–748, Sept. 1981.

[8] ——, "High angular microwave resolution from a distorted array," *Proc. 1980 Int. Comput. Conf.*, vol. 231, pp. 150–156, Apr. 1980.

[9] R. S. Berkowitz and E. N. Powers, "TASAR, a thinned adaptive synthetic aperture radar," IEEE EASCON '78 Rec., Arlington, VA, IEEE Pub. 78 CH 1354-4 AES, pp. 135–142.

[10] G. T. Ruck, Ed., *Radar Cross Section Handbook*. New York: Plenum, 1970.

[11] R. S. Berkowitz, Ed., *Modern Radar Systems*. New York: Wiley, 1965.

Bernard D. Steinberg (S'48–A'50–SM'64–F'66), for a photograph and biography please see page 748 of the September 1981 issue of this TRANSACTIONS.

Distributed Airborne Array Concepts

...NBERG, Fellow, IEEE

...IEEE

The ... and detection range due to distributing ... antenna array throughout the airframe and skin of an aircraft is examined. SNR formulas for three system configurations are presented and compared with that of a conventional, monostatic radar. Examples given in the paper show detection range increases as large as a factor of 4. Three additional potential advantages of the distributed array are an increase in spatial signal processing capability, an improvement in azimuthal resolution, and a potential reduction in transmitter power for fixed radar performance so as to reduce the probability of intercept.

Manuscript received September 5, 1980; revised April 15 and September 14, 1981.

This work was supported by the Air Force Office of Scientific Research under Grant AFOSR-78-3688.

Authors' address: B. Steinberg, Valley Forge Research Center, Moore School of Electrical Engineering, Philadelphia, PA 19104; E. Yadin, Interspec Inc., Philadelphia, PA 19104.

18-9251/82/0300-0219 $00.75

INTRODUCTION

Radar performance in noise and jamming is a monotonic function of the power-aperture product [1, 2]. This paper evaluates the improvement in radar performance due to increasing the aperture size of airborne radar by distributing antenna elements or small subarrays throughout large portions of the skin of an aircraft. The performance measure adopted is signal to receiver noise ratio (SNR) and its equivalent, detection range of targets in noise.

The critical technical problem is that of overcoming the distortion in such a phased array due to the nonrigidity of the skin and airframe. This problem is introduced (but not solved) in the paper, and a discussion of other difficult technical problems is presented. The problem of nonrigidity must be overcome by a retrodirective [3, 4], self-adaptive technique [5, 6, 7] based upon echoes from land or sea clutter.

In addition to enhanced SNR and detection range, increasing the size of the aperture to include all or most of the airframe offers the advantages associated with small beamwidth.

One important advantage has to do with protection against jammers that are close to the axis of the beam. Rejection of jamming energy by low sidelobe design or adaptive techniques such as coherent sidelobe cancellation and adaptive nulling [8-12] are known and useful techniques. Main lobe jamming, however, is not suppressed without hazarding the suppression of target return. Increasing the size of the aperture reduces the width of the main lobe and thereby reduces the minimum angular separation between target and jammer at which sidelobe suppression techniques can operate.

A second advantage of the reduced beamwidth is the enhanced potential for target counting and classification.

An additional value of the improved detection performance is the possibility of a drastic reduction in transmitter power for a given performance so as to permit the successful design of a low probability of intercept radar.

The paper focuses upon the SNR performances of three airborne distributed array systems as compared with that of a conventional radar with a modest sized, confined antenna used both for transmitting and receiving. From the parametric relations that are developed, the conditions which produce superior detection performance can be determined. Generally speaking, it is found that the larger the aircraft and the shorter the wavelength, the greater the potential benefit. In one X-band design a potential increase in detection range by a factor of 4 is reported.

NOMENCLATURE

P	Average transmitted power in watts.
G_T	Transmitter antenna gain.
A_R	Receiving antenna area in meters squared.
λ	Wavelength in meters.
T_o	Integration time in seconds.
o	Target cross section in meters squared.
R	Target to radar distance in meters.
k	Boltzmann's constant (1.38×10^{-23} joules per degree Kelvin).
T	Reference temperature (290 degrees Kelvin).
M	Total system and propagation loss factor (including receiver noise figure, integration loss, antenna efficiency loss, filter matching loss, etc.). Subscripts are used in the text to distinguish between the systems.
θ	Azimuth beamwidth in radians.
θ_s	Azimuthal surveillance sector in radians.
ϕ	Elevation beamwidth in radians.
ϕ_s	Elevation sector in radians.
D	Width of high gain antenna in meters.
L	Length of aircraft in meters.
W	Width of strip available on the fuselage for the distributed antenna array in meters.
η	Deployment efficiency (fraction of available fuselage area used as electromagnetic transducer).
T_s	Scan time in seconds.
N	Number of antenna elements.
P_e	Average power radiated by individual element in watts.
A_e	Element aperture in meters squared.

MONOSTATIC RADAR WITH ROTATING TRANSMIT-RECEIVE ANTENNA

This is the reference system against which the distributed antenna systems are compared. Examples are the E-2 and E-3 airborne early warning (AEW) systems. The integrated output SNR is given by [2]

$$\text{SNR} \triangleq r = PG_TA_R\sigma T_o/(4\pi)^3R^4kTM. \quad (1)$$

The azimuth beamwidth $\theta = \lambda/D$. The antenna gain is given by $G_r = 4\pi/\theta\phi = 4\pi D/\lambda\phi$. The receiving antenna area is given by $A = \lambda D/\phi$. It is assumed that the integration time T_o is equal to the time on target (time during which the target is illuminated). That time is less than T_s by the ratio of azimuthal beamwidth to 2π, or $T_o = \lambda T_s/2\pi D$ where the scan time T_s is the time for a mechanically scanning antenna to rotate 2π rad. Making these substitutions yields

$$r = P\lambda\sigma DT_s/8\pi^2\phi_s^2R^4kTM_1 \quad (2)$$

where the subscript 1 has been given to M to designate system 1. The elevation beamwidth ϕ of the antenna is assumed to be equal to the desired elevation coverage ϕ_s.

DISTRIBUTED RECEIVING ARRAY AND HIGH GAIN ROTATING TRANSMITTING ANTENNA

Fig. 1 shows how the reference system is modified. The high gain rotating antenna is retained but is used only for transmission. The receiving system is a distributed array; a fuselage array is depicted in the figure. It consists of N receiving elements distributed in a band along the length of the fuselage. Let the length of the fuselage be L and the width of the band be W (e.g., L and W for a Boeing 707 are approximately 45 m and 2 m). The receiving array is distributed along the aircraft surface forming an aperture of length $L \gg D$; hence the receiving beamwidth is much smaller than the transmitting beamwidth. To prevent diminishing the number of hits per target, the signal processor simultaneously forms a group of adjacent receiving beams to fill the transmitting main beam. The number of receiving beams will be $\theta_T/\theta_R = L/D$, where θ_T is the transmitting beamwidth and θ_R is the receiving beamwidth. The elevation beamwidth of the receiving array (λ/W) is usually much narrower than the required elevation coverage ϕ_s. Hence $W\phi_s/\lambda$ receiving beams in elevation must be formed to cover the desired sector ϕ_s.

Number of Receiving Elements

The element radiation pattern should cover the desired surveillance sector of the radar. Therefore it should have a beamwidth of θ_s in azimuth and ϕ_s in elevation. The width and length of each array element are, therefore, $D_1 = \lambda/\theta_s$ and $D_2 = \lambda/\phi_s$, respectively. The fuselage area available for deploying the elements is $L\ W$. If we assume that a fraction $\eta < 1$ of that area is used for the electromagnetic transducer, then the number of antenna elements in the fuselage array becomes

$$N = \eta LW/D_1D_2 = \eta LW\theta_s\phi_s/\lambda^2. \quad (3)$$

Equation (3) is evaluated for two different aircrafts and the results are given in Table I. One airplane is the Boeing 707, a large aircraft which could serve an AEW function; the other is a smaller, high-performance aircraft such as the General Dynamics F-16. L and W for these aircraft are approximately 45 m and 2 m, and 10 m and 1 m, respectively. In both cases $\eta = 0.5$ is assumed. Taking the azimuthal surveillance sector $\theta_s = 2$ rad and the required elevation coverage $\phi_s = 1$ rad, the number of elements is shown in Table I.

The SNR is derived by substituting the proper area A in (1). A is given by NA_e. The effective element area A_e is given by $\lambda^2/\phi_s\theta_s$. G_T is given by $4\pi D/\lambda\phi_s$. N is given by (3), and T_o by $\lambda T_s/2\pi D$. Substitution yields

$$r = \eta P_o L W T_r / 8\pi^2 \phi_r R^4 k T M_2. \quad (4)$$

It is interesting to observe from (4) that the signal to noise power ratio is not affected by the transmitting azimuth beamwidth. This is true provided that the beamwidth does not get so large that it is no longer possible to integrate coherently across the beam. In that case integration must be partially coherent and partially noncoherent, and the integration loss increases, a factor affecting the performance of system III. This is discussed numerically in a later section. Also discussed there are the relative beamshape losses. Another relevant factor in comparing the systems is that even though the SNR might not be influenced by azimuth transmitting beamwidth, the number of receiving beams is affected by the beamwidth; hence the size of the transmitting antenna affects the complexity of the signal processor.

DISTRIBUTED RECEIVING ARRAY AND LOW GAIN NONROTATING TRANSMITTING ANTENNA

In this design the high gain rotating transmitting antenna is eliminated and one of the array elements is substituted as a low gain, wide beam transmitter. The azimuthal width of the transmitting antenna pattern becomes equal to θ_r. Its elevation beamwidth ϕ_r is unchanged. Therefore, $G_T = 4\pi/\phi_r\theta_r$. The receiving antenna is formed from N such antenna elements. Therefore, $A = NA_r = N\lambda^2/\theta_r\phi_r$. Substituting (3) for N yields $A = \eta LW$.

To achieve the maximum integration gain, the signal processor simultaneously forms a group of adjacent receiving beams such that the azimuthal sector covered by the receiving beams is the same as that of the transmitting pattern. Hence, the integration time T_o will be longer than in designs I and II, which compensates for the low gain of the transmitting antenna. The relative efficiencies are discussed in a later section. As a result of the increased integration time, the integration loss also will be increased. M_3 can be used to indicate this increased loss. As in system II, $W\phi_r/\lambda$ receiving beams in elevation are formed simultaneously to cover the desired sector ϕ_r. For generality the transmitter power will be indicated by P'. Making these substitutions results in

$$r = \eta P' \sigma L W T_o / 4\pi\theta_r\phi_r R^4 k T M_3. \quad (5)$$

DISTRIBUTED TRANSMITTING AND RECEIVING ARRAY

Here it is assumed that each element transmits and receives. The average power transmitted per element is P_r and the element gain is G_r. The average power density at the target due to a single transmitter element is $W_r = P_r G_r / 4\pi R^2$. The electric field E_r is proportional to $W_r^{1/2}$. When the transmitting array is focused on a target the total electric field is $E = N E_r$ and the total average power density is $W = N^2 W_r$. Therefore the SNR at the receiver is

$$r = (N^2 P_r G_r)\sigma(NA_r) T_o^- / (4\pi)^2 R^4 k T M_4 \quad (6)$$

where NA_r is the total receiving aperture and T_o^- is the integration time. In this design electronic scan in azimuth and elevation for both transmit and receive beams is required. The ratio T_r/T_o^- is equal to the number of transmit-receive beams within the surveillance sector θ_r, ϕ_r. Therefore $T_o^- = \lambda^2 T_r / LW\theta_r\phi_r$. For this design integration losses can be ignored since $T_o^- \ll T_r$. (Care must be taken that T_o^- is not less than one interpulse period, however, a condition which the equation above may lead to at the shorter wavelengths. In such a case T_r must be lengthened or the other parameters decreased so that at least one hit per target is available to each beam.) The gain and aperture area of an element is the same as G_r, A_r in design III. N is given by (3). Hence $NA_r = \eta LW$ and $T_o^- = \eta T_r / N$. Making these substitutions yields

$$r = \eta^2 N P_r \sigma L W T_r / 4\pi\theta_r\phi_r R^4 k T M_4. \quad (7)$$

Fig. 1. Distributed receiving array and high gain rotating transmitting antenna.

TABLE I
Number of Elements Deployable Along One Side of the Fuselage, $\eta = 0.5$

Wavelength (m)	Aircraft	N
0.3	Boeing 707	1000
0.1	Boeing 707	9000
0.03	General Dynamics F-16	11000

SNR IMPROVEMENT FACTOR

The ratios of (4), (5), and (7) to (2) are the relative SNRs of the three distributed array systems to the conventional, monostatic radar. This ratio, designated the relative gain or improvement factor I, is given in the first column of Table II.

The second column of Table II is based on four assumptions: 1) the angular sector θ_r is assumed to be about 2 rad; 2) the required elevation coverage is

TABLE II
SNR Gains of Systems II, III, and IV Relative to System I

System	SNR Improvement Factor I	
	General Case	Special Case, $\theta_s = 2$ rad, $\phi_s = 1$ rad, $T_0' = T_r$, $P'/P = NP_e/P = \theta_e/2\pi$
II	$\eta M_1 \phi_s LW/M_2 \lambda D$	$\eta M_1 LW/M_2 D$
III	$2\pi\eta M_1 P' T_0' \phi_s LW/M_3 P\theta_s T_r \lambda D$	$\eta M_1 LW/M_3 \lambda D$
IV	$2\pi\eta^2 M_1 NP_e \phi_s LW/M_4 P\theta_s \lambda D$	$\eta^2 M_1 LW/M_4 \lambda D$

about 1 rad; 3) $T_0' = T_r$, which implies that the rate at which target data are delivered to the user is the same for all systems; 4) $P'/P = NP_e/P = \theta_e/2\pi$, which implies the use of the same power per angular sector for all systems. It is seen that for all distributed designs I increases linearly with $LW\phi_s/\lambda D$. LW is the fuselage area (one side) and $\lambda D/\phi_s$ is the aperture of the conventional fuselage area (one side) and $\lambda D/\phi_s$ is the conventional antenna used in design I. $LW\phi_s/\lambda D$, therefore, is the maximum potential increase in aperture. Since η is the fraction of the fuselage area used to deploy the elements, $\eta LW\phi_s/\lambda D$ is the factor by which aperture increases. It is shown later that system losses M_2, M_3, and M_4 are larger than the loss M_1 of the conventional design (i.e., the fractions M_1/M_2, M_1/M_3, M_1/M_4 are smaller than unity). Hence the aperture gain $\eta LW\phi_s/\lambda D$ must be significantly higher than unity to make the distributed designs attractive.

RELATIVE SYSTEM LOSSES

The parameters M_2/M_1, M_3/M_1, and M_4/M_1 represent total system and propagation losses for designs II, III, and IV relative to the conventional design I. The contributions to the system loss are compared below. Propagation losses are unaffected by choice of design.

Beam-Shape Loss

As the beam scans over a target, the echo pulses are modulated by the antenna pattern, reaching the maximum value only when the beam points directly at the target. Blake [16, 17] showed that antenna modulation represents a loss of SNR of 1.6 dB for an antenna scanning in one dimension and a 3.2 dB loss when a pencil beam is used to scan in two dimensions. When the number of hits per scan is very low, the average loss will increase because the target might be seen only at the edge of the beam. The pattern loss for these cases are given in [18].

For the purpose of this analysis it is assumed that the conventional design (system I) has a pattern loss of 1.6 dB (0.8 dB for transmission and 0.8 dB for reception).

Design II, using the mechanically scanned transmitting antenna and the electronically scanned multiple narrow beams for receiving, has the same modulation effect both for transmitting and receiving. Therefore, the pattern loss for this design is the same as that of system I.

System III also uses multiple receiving beams. Here the receiving beams are stationary, but since they are very narrow, aircraft and target motion cause target echos to move through several receiving beams during the integration time. This is equivalent to scanning the receiving beams over the target. Therefore a pattern loss of 0.8 dB for reception is assumed.

The broad transmitting beam in system III also is stationary. Its power pattern $G_T(\phi)$ is angle dependent. Its maximum value is at $\theta = 0$ and it drops by 3 dB for $\theta = \pm \theta s/2$. The beam-shape loss for this case is defined as the additional SNR required to maintain the same average probability of detection P_d as for the loss-free case.

The SNR depends linearly on $G_T(\theta)$. Since P_d is a function of SNR, it also is angle dependent, i.e., $P_d = g(\theta)$. If we assume that targets are uniformly distributed in angle throughout the surveillance sector θ_s, then the average probability of detection is given by

$$\overline{P}_d = \theta_s^{-1} \int_{\theta-\theta s/2}^{\theta+\theta s/2} g(\theta)\, d\theta. \tag{8}$$

It is further assumed that in the interval $-\theta s/2 < \theta < \theta s/2$ the one-way power pattern and, therefore, the SNR can be approximated by a constant times $\cos^2(2\pi\theta/2\theta_s)$. The nonlinear dependence of P_d on SNR is calculated in many radar handbooks for different false alarm rates. By using P_d (SNR) given in [1, ch. 2, fig. 4], (8) was evaluated. For a 2 rad surveillance sector and a constant probability of false alarm of 10^{-6} it was found that an SNR of 14.3 dB is required to achieve an average probability of detection of 0.9. Comparing that with the required 13.2 dB SNR associated with the loss-free case and the same probability of detection, it is concluded that the beam-shape loss for transmitting is 1.1 dB. Therefore a total of 1.9 dB beam-shape loss is assumed for design II.

Design IV involves two dimensional scanning for which the loss is 3.2 dB provided that there is more than one hit per scan. In addition, the transmitting gain for each element has the same angle dependence as in design III. Therefore an additional loss of 1.1 dB is added. A total beam-shape loss of 4.3 dB is assumed for this design. Based on this analysis the estimated relative (to design I) beam-shape losses are 0

dB, 0.3 dB, and 2.7 dB for designs II, III, and IV, respectively.

Integration Loss

The integration losses are expected to be negligible for designs I, II, and IV because their integration times will be short enough to allow coherent integration with negligible losses. The integration time for each is limited by the beamwidth of the transmitting antenna or the transmitting array and by the required scanning time through the sector. In design III, however, the total sector is continuously illuminated by the broad beamwidth, nonrotating transmitting antenna. The integration time will be limited only by the required rate at which data are to be delivered to users. Since integration over a few thousand pulses (several seconds) is expected to take place in design III, some combination of coherent and noncoherent integration will be required. Hence, integration loss relative to ideal coherent integration cannot be ignored. As an example, an integration loss of ~ 2.5 dB is expected for a mixed integration process having a 2000 pulse integration time when coherent integration of only 100 pulses is possible [2, pt. IV, ch. 4].

Receiver Noise Figure

There is no reason why the receiver noise figures should differ in the four designs.

Adaptive Beam-Forming Loss

It is explained later that the three distributed array designs will probably require adaptive self-cohering techniques to compensate for fuselage vibrations. Calculating the loss in the self-cohering procedure is beyond the scope of this paper. However, experience with experimental adaptive beam-forming and scanning systems at the Valley Forge Research Center [13] indicates that the one-way loss can be held below 1 dB. This value will be attributed to designs II and III and a 2 dB loss will be attributed to design IV.

Combined Relative Losses

These estimates are used in the performance examples given below. Expressed in decibels, the ratios of the loss factor M_t to the losses in systems II, III, and IV are -1dB, -3.8dB, and -4.7dB.

INCREASE IN SNR AND DETECTION RANGE

In comparing the four systems it is tempting to assume either that their average powers are equal or that their average powers per unit azimuthal angle are equal. However, such assumptions are not necessarily realistic. P and NP_t are affected by, and therefore limited by, different physical and design phenomena. NP_t can be larger or smaller than P. Because of the large possible range in their ratio it is fruitless to take it into account in comparing the relative merits of the systems. Thus, only the effect of the enhanced aperture is included in our discussion.

TABLE III
SNR Gains in Decibels of Systems II, III, IV Relative to System I Due to Enlarged Aperture of Distributed Array

System	L-Band AEW on Boeing 707	S-Band AEW on Boeing 707	X-Band on General Dynamics F-16
II	13.2	18.5	23.9
III	10.4	15.7	21.1
IV	6.5	11.8	17.2

TABLE IV
Ratios of Detection Ranges of Systems II, III, IV to System I

System	L-Band AEW on Boeing 707	S-Band AEW on Boeing 707	X-Band on General Dynamics F-16
II	2.14	2.90	3.96
III	1.82	2.47	3.37
IV	1.45	1.97	2.69

Table III shows the SNR improvement factors due to the enlarged aperture of the distributed array and Table IV shows the factors by which the detection ranges increase for $\theta_t = 2$ rad, $\phi_t = 1$ rad, $T_0' = T_0$, $P'/P = NP_t/P = \theta_t/2\pi$, $\eta = 0.5$ and for three sets of parameters: 1) $D = 20\lambda$, $L = 150\lambda$, $W = 7\lambda$; 2) $D = 50\lambda$, $L = 450\lambda$, $W = 20\lambda$; 3) $D = 20\lambda$, $L = 350\lambda$, $W = 35\lambda$. The first two sets are realistic for L- and S-band ($\lambda = 0.3$ and 0.1 m) AEW radar on a large aircraft such as a Boeing 707; the third set is realistic for an X-band ($\lambda = 0.03$ m) radar on a small aircraft such as a General Dynamics F-16. The value 0.5 chosen for η is based upon examination of aircraft models and photographs and may prove somewhat optimistic. For $\eta = 0.25$, systems II and III lose 3 dB in SNR gains and system IV loses 6 dB.

The SNR gains of systems II, III, and IV relative to system I (shown in Table III) are also equal to the amount by which the total transmitted powers of the distributed systems can be decreased while maintaining the same detection range as the conventional system.

AN AEW EXAMPLE

Consider the long range detection problem with the following radar and target parameters:

TABLE V
Average Transmitted Power Required to Achieve 650 km Detection Range

System	$\eta = 0.1$	$\eta = 0.2$	$\eta = 0.3$	$\eta = 0.4$	$\eta = 0.5$
I	83 kW (not a function of η)				
II	5.86 kW	2.93 kW	1.95 kW	1.46 kW	1.17 kW
III	11.15 kW	5.58 kW	3.72 kW	2.79 kW	2.23 kW
IV Total	136.98 kW	34.25 kW	15.22 kW	8.56 kW	5.48 kW
per module	76 W	9.51 W	2.82 W	1.19 W	0.61 W

$\sigma = 10\ m^2$ $W = 2$ m

$f_r = 200$ Hz $\eta = 0.5$

$\lambda = 0.1$ m $P'/P = NP_e/P = \theta_e/2\pi$

$D = 50\lambda$ $M_1/M_2 = -1.0$ dB

$L = 45$ m $M_1/M_3 = -3.8$ dB

$kT = 4 \times 10^{-21}$ W/Hz $M_1/M_4 = -4.7$ dB

$M_1 = 10$ dB SNR = 13 dB (corresponding to 0.95 probability of detection and 10^{-6} probability of false alarm)

$T_0' = T_r = 10$ s

$\phi_e = 1$ rad

$\theta_e = 2$ rad

$R = 650$ km (desired detection range).

The average transmittted power required to achieve 650 km detection range for the four systems is shown in Table V for several different values of element deployment efficiency η. The differences are dramatic. Whereas an unrealistic 83 kW is required for the conventional, monostatic design, less than 5 kW suffices for a bistatic system with a large, distributed receiving array.

SIDELOBE LEVEL OF A RANDOM ARRAY

One of the important parameters in system performance is the average sidelobe level (ASL) of the array in the receiving mode, which is $1/N$ [7]. The pattern of the transmit-receive array is the square of the radiation pattern of the distributed receiving array and, hence, ASL for this case is $1/N^2$. The factor of N advantage is of considerable importance in detecting targets in clutter, which, therefore, makes system IV preferred over systems II and III. However, the improved two-way sidelobe pattern is of no advantage with respect to jamming; all systems will perform according to the $1/N$ ASL of the receiving array. Since the one-way average sidelobe level is not likely to be less than -35 dB, other electronic counter-countermeasure techniques must be designed into such a system. Adaptive nulling is very attractive in this regard [10, 12, 15].

POTENTIAL FOR HIGH ANGULAR RESOLUTION

The minimum available beamwidth of an aperture of length D operating at wavelength λ is the order of λ/D rad. As an example, the typical horizontal aperture of an X-band nose-mounted radar antenna is 20 wavelengths. Its beamwidth is 1/20 rad or 3°. At a radar distance of 20 km the beam cross section is 1 km. The beamwidth of the radar in the Boeing E-3A Airborne Warning and Control System (AWACS) is the order of 1°.

Now imagine that the receiving aperture is spread over the airframe. The effective size for any direction of view is the projected length of the airplane as seen from that direction (Fig. 2). The effective length for most aircraft is close to the length of the fuselage or the wing span regardless of direction. The fuselage of the Boeing 707 is 45 m in length. An aperture of this size at L-band (30 cm) is 150 wavelengths. The beamwidth would be 1/150 rad = 6.7 mrad = 0.38°. Table VI gives the beamwidths at several wavelengths and includes the resolving power of human optics for comparison.

It is seen that the optical resolution of the radar operator, with his eyes and brain, is the same order as the potential resolution of a distributed array installed on a large aircraft and operated at the shorter radar wavelengths. Thus, the potential exists for providing him with an all weather, all around looking, night and day, microwave imaging system with as fine a resolution as he himself has with his eyes and brain.

PHASE SYNCHRONIZING THE DISTRIBUTED ARRAY

The fundamental problem of cohering or phase synchronizing the array is that the airframe is not rigid and that its skin vibrates. The problem is less serious at L-band than at X-band because the positional tolerance ($\lambda/4\pi$) is 10 times larger. Nonetheless techniques which compensate for element position uncertainty will be needed if the bulk of the entire airframe is to be available for the radar array. It is expected that self-cohering or adaptive beam forming

will be required. A method suitable for airborne use for systems II an III is described in [7]. It is a self-cohering process which forms a retrodirective [3, 4] beam upon echoes from land or sea clutter. The search algorithm for obtaining the reference signal for the adaptive beam forming process is described in [5, 6]. Early experimental results using this algorithm are given in [13, 19]. The transmit-receive problem (system IV) is much more complicated. Active retrodirective techniques have been designed for the solar power satellite (SPS) concept [14].

OTHER PROBLEMS

Many other problems confront the designer, although none so fundamental as the one above. The companion problem to the adaptive phase synchronization problem is scanning the receiving array following adaptive beam forming. This problem has been solved [13, 14]. The tolerance theory regarding element position uncertainty is understood [7]. The next major problem is the development of methods of adaptive beam forming of a transmitting array on a moving aircraft. The SPS work already done will be helpful [14]. Some of the other design problems are those typical of phased array designs (types of elements, single elements versus subarrays or clusters, methods of mounting, polarization, and bandwidth) while others relate specifically to the self-cohering system (methods of phase conjugation and reference phase distribution for adaptive transmit-receive array, effects of multipath and scattering from the ground or sea surface and from reflections within the array from the aircraft structure, interconnections between elements and the signal processor, real time adaptive signal processing, and display).

OBSERVATIONS REGARDING SNR AND DETECTION RANGE

The results shown in the tables are very attractive. They indicate that the distributed airborne array will be useful when large detection range with low transmitted power is required. In addition, the distributed airborne array is useful when adaptive nulling close to the beam axis and better angular resolution are desired.

In systems I, II, and III a single transmitter radiates the full power. System III, using a single low gain nonrotating antenna, is far superior to the other two mechanically but requires a more complicated signal processor to simultaneously form many receiving beams in azimuth as well as in elevation. In addition, it must provide efficient integration over T_o. In SNR performance, system III is slightly poorer (about 3 dB) than system II. However, by not requiring the massive rotating antenna used in II, the third design is more attractive. System IV radiates from the distributed array. It is a much more complicated system than system III, but it offers a very much lower two-way sidelobe level. It exhibits SNR and detection range poorer than designs II and III for the same total transmitted power. SNR performance (relative to designs II, III) decreases linearly with the deployment efficiency factor η. Differences of nearly 4 dB and 11 dB in SNR performances relative to design III are estimated for $\eta = 0.5$ and $\eta = 0.1$, respectively. Therefore design IV is preferred only if the reduced two-way sidelobe level is essential.

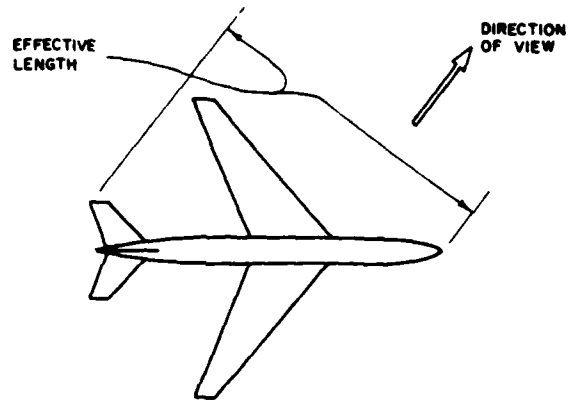

Fig. 2. Effective array length is projected extent of aircraft normal to direction of view.

TABLE VI
Beamwidths of a 45 m Aperture and the Human Optical System

Physical Aperture	λ(m)	Beamwidth (mrad)
Boeing 707	3×10^{-1}	6.7
Boeing 707	3.2×10^{-2}	0.7
Boeing 707	8.6×10^{-3}	0.2
Human eye	5×10^{-7}	0.3

SUMMARY

The improvement in SNR and detection range due to distributing an antenna array throughout the airframe and skin of an aircraft is examined. SNR formulas for three system configurations are presented and compared with that of a conventional, monostatic radar. Each of the new systems uses the distributed array for reception. One of them uses a separate, high gain, rotating transmitting antenna while another uses one of the receiving antenna elements for transmission. Both designs are bistatic. The third new system uses the entire distributed array for transmission.

SNR and detection range performances for each of the three distributed systems exceed those of conventional, monostatic radar. The *X*-band example given in the paper shows a potential detection range increase as large as a factor of 4.

In addition to the dramatic performance increase expected from the distributed array, it offers three additional potential advantages: an increase in spatial signal processing capability because of the enlarged size of the aperture, an improvement in azimuthal resolution, and a potential reduction in transmitter power for fixed radar performance so as to reduce the probability of intercept.

The critical problem to be solved is that of phase synchronizing the distributed array when the airframe is nonrigid.

REFERENCES

[1] Skolnik, M.I. (Ed.) (1970)
Radar Handbook.
New York: McGraw-Hill, 1970.

[2] Berkowitz, R.S. (Ed.) (1965)
Modern Radar.
New York: Wiley, 1965.

[3] Special issue on "Active and Adaptive Antennas."
IEEE Transactions on Antennas and Propagation, Mar. 1964. *AP-12*, 140-246.

[4] Hansen, R.C. (Ed.) (1964)
Microwave Scanning Antennas, vol. 3.
New York: Academic Press, 1964, ch. 5.

[5] Steinberg, B.D. (1980)
High angular microwave resolution from distorted arrays
Proceedings of the 1980 International Computing Conference vol. 23.
Washington, D.C., Apr. 1980.

[6] Steinberg, B.D. (1981)
Radar imaging from a distorted array: the radio camera algorithm and experiments.
IEEE Transactions on Antennas and Propagation, Sept. 1981, *AP-29, 740-748.*

[7] Steinberg, B.D. (1976)
Principles of Aperture and Array System Design.
New York: Wiley, 1976.

[8] Howells, P.A. (1965)
Intermediate frequency sidelobe canceler.
U.S. Patent 3-202-990, Aug. 1965.

[9] Applebaum, S.P. (1966)
Adaptive arrays.
Syracuse University Research Corp., Report STLSPL TR 66-1, Aug. 1966.

[10] Widrow, B., et al. (1967)
Adaptive antenna systems.
Proceedings of the IEEE, 55, Dec. 1967, 2143-2159.

[11] Brennan, L.E., and Reed, I.S. (1973)
Theory of adaptive radar.
IEEE Transactions on Aerospace and Electronic Systems, Mar. 1973, *AES-9,* 237-252.

[12] Gabriel, W. (1976)
Adaptive array—an introduction.
Proceedings of the IEEE, Feb. 1976, *64,* 239-272.

[13] Steinberg, B.D., et al. (1979)
First experimental results from the Valley Forge radio camera program.
Proceedings of the IEEE (Letters), Sept. 1979, *67, 1370-1371.*

[14] Chernoff, R. (1979)
Large active retrodirective arrays for space applications.
IEEE Transactions on Antennas and Propagation, July 1979, *AP-27,* 489-496.

[15] Applebaum, S.P. (1976)
Adaptive arrays.
IEEE Transactions on Antennas and Propagation, Sept. 1976, *AP-24,* 585-598.

[16] Blake, L.V. (1953)
The effective number of pulses per beamwidth for a scanning radar.
Proceedings of the IRE, June 1953, *41,* 770-774.

[17] Blake, L.V. (1953)
Addendum to "pulses per beamwidth for radar".
Proceedings of the IRE (Correspondence), Dec. 1953, *41,* 1785

[18] Hall, W.M., and Barton, D.K. (1965)
Antenna pattern loss factor for scanning radars.
Proceedings of the IEEE (Correspondence). Sept. 1965, *53,* 1257-1258.

[19] Steinberg, B.D., and E. Yadin (1982)
Radio camera experiment with airborne radar data *Proceedings of the IEEE* (Letters), Jan. 1982, 67, 96-98.

Bernard D. Steinberg (S'48—A'50—SM'64—F'66) was born in Brooklyn, NY in 1924. He received the B.S. and M.S. degrees in electrical engineering from the Massachusetts Institute of Technology, Cambridge, in 1949 and the Ph.D. degree from the University of Pennsylvania, Philadelphia, in 1971.

He worked in the Research Division of Philco through the middle 1950's, specializing in radar backscatter and radar signal processing. He was one of the founders of General Atronics Corporation in Philadelphia in 1956 and served as its Vice President and Technical Director for 15 years. His work there was in signal processing techniques and their applications to radar, HF communications, hydroacoustics, and seismology. His most recent work is in self-adaptive signal processors, particularly in large antenna arrays. Since 1971, he has been a Professor with the Moore School of Electrical Engineering at the University of Pennsylvania, Philadelphia, and Director of its Valley Forge Research Center, where he is engaged in development of a large self-adaptive microwave imaging system called the Radio Camera. He is the author of *Principles of Aperture and Array System Design* (Wiley, 1976), in which early radio camera concepts are described, and currently is preparing a detailed book on the subject. He also is a consultant in the Airborne Radar Branch of the Naval Research Laboratory.

Dr. Steinberg is a member of U.S. Commissions B and C of the International Scientific Radio Union (URSI).

Eli Yadin (S'79) was born in Haifa, Israel, in 1950. He received the B.S. degree in electrical engineering from Technion—Israel Institute of Technology, Haifa, in 1972 and the M.S. degree in electrical engineering from Tel Aviv University in 1978. He recently completed the Ph.D. dissertation in systems engineering at the University of Pennsylvania, Philadelphia, 1981.

From 1972 through 1977 he was a military and electronic systems engineer in the Israeli Air Force where he was involved in areas of radar and fire control systems. From 1978 through 1981 he was a graduate student and held a research fellowship at the University of Pennsylvania. His recent research work is in the area of large self-adaptive antenna arrays. He is now employed by Interspec, Inc., Philadelphia, PA.

Radio Camera Experiment with Airborne Radar Data

BERNARD D. STEINBERG AND ELI YADIN

Abstract—**The radio camera signal processing algorithm for retrodirective adaptive beamforming and scanning is demonstrated to work successfully on radar clutter echoes. The experiment was conducted with airborne radar data obtained from the Naval Research Laboratory.**

A radio camera is an imaging radar with too large an aperture to ensure that the aperture is mechanically stable. Retrodirective adaptive beamforming techniques are used to cohere or phase-synchronize the array. The receiving beam, after it is self-cohered upon the reradiation from some target outside of the array, can be scanned in angle by conventional, open-loop phased array techniques.

The first experimental radio camera demonstration of high angular resolution imaging appeared in 1979 [1]. In that experiment, a highly distorted, 27-m array, consisting of 100 randomly located sample points, self-cohered on the backscatter from a corner reflector at 210 m. The experiment was conducted at X-band. Thirty meters more

Manuscript received July 29, 1981. This work was supported by the Naval Research Laboratory and the Air Force Office of Scientific Research.

The authors are with the Valley Forge Research Center, Moore School of Electrical Engineering, University of Pennsylvania, Philadelphia, PA 19104.

0018-9219/82/0100-0096$00.75

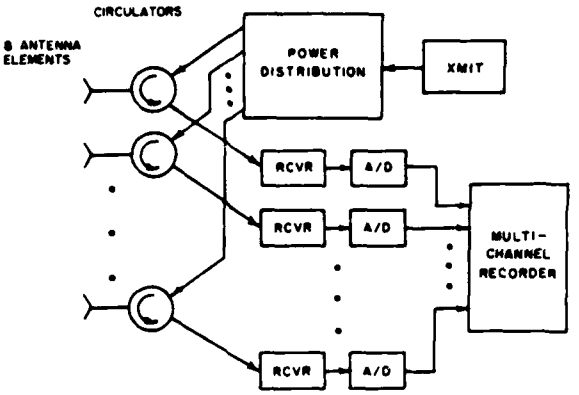

Fig. 1. NRL experimental equipment.

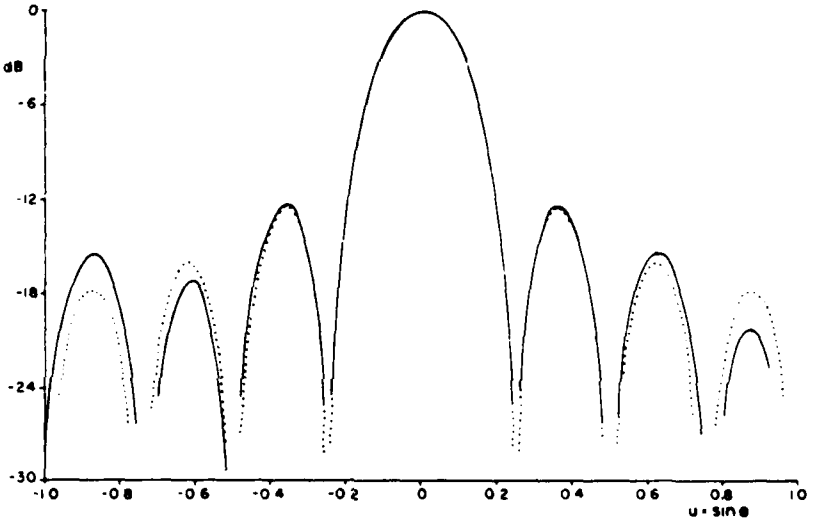

Fig. 2. Comparison of patterns formed adaptively (solid) and non-adaptively. Beam direction is near ground track of aircraft.

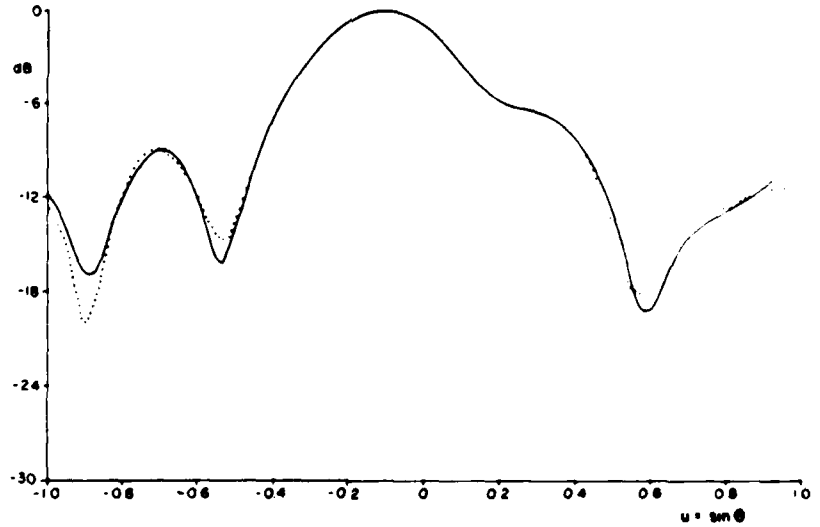

Fig. 3. Comparison of scanned outputs of adaptively (solid) and non-adaptively formed beams.

distant was a target group consisting of two corner reflectors. The beamforming reflector and the target reflectors both were in the near field of the array. In the experiment the adaptively formed beam was refocused to the target range and scanned in angle across the target. The resulting image was indistinguishable from the calculated response of the system when operating in free space.

The experiment reported in this letter used airborne radar data obtained from F. Staudaher of the Naval Research Laboratory. An 8-element UHF phased array was flown at 200 knots at an altitude of 15 000–20 000 ft over the southeastern portion of the U.S. The transmitting pattern was Dolph–Chebyshev-weighted for -24 dB sidelobes. The received radar echoes were separately recorded on each of the 8 channels in a specially designed, high quality digital recording system. Demodulation was coherent and the in-phase and quadrature video channels were recorded with 10 bit precision. A functional sketch is shown in Fig. 1.

One object of the experiment was to test whether the radio camera algorithm would operate successfully upon ground clutter. Since the array was rigid, its proper performance could be predicted and, hence, compared to the performance of the adaptive system.

The radio camera algorithm used in the experiment is described in [2]. The algorithm consists of three parts. First, the variance of the amplitudes of the group of echoes from each range bin is measured. The range bin having the lowest echo variance, when normalized to the average echo power in that range bin, is selected as the reference range for the system. Next, the processor either multiplies the complex sample at each array element from each range trace by the complex conjugate of the echo at the reference range or, more simply, merely phases rotates the received echoes by the phases of the complex conjugates of the signals at the reference range. This is the adaptive part of the process. Lastly, the processor applies linear phase weighting across the array to electronically scan the adaptively formed beam in angle.

The object of the first step is to find a target or a clutter patch whose reradiation most closely approximates that of the point source. The object of the second step is to self-cohere the array upon that target. The object of the third step is to scan the beam in angle to the left and right of that target.

The solid curve of Fig. 2 shows the pattern which resulted from the adaptive process. As is explained in [3], the beam which is formed by the adaptive procedure is directed toward the dominant scattering center in the illuminated ground patch in the range bin selected by the signal processor for adaptive beamforming. Hence, the origin will usually differ from the bearing of the transmitting array. In this experiment the difference turned out to be 0.07 rad or $\sim 0.3\ \lambda/L$ (λ = wavelength, L = antenna length). The bearing of the transmitting array was fixed at 0.6° from the flight direction. The dashed curve shows the receiving pattern of a uniformly weighted 8-element array associated with conventional nonadaptive beamforming. The origin of that pattern which is the bearing of the transmitting array has been shifted by 0.07 rad so that the adaptive and nonadaptive patterns can be compared. The results are very similar, indicating that the adaptive process worked well. The smallest echo variance observed was 0.0026.

Satisfactory results have been obtained when the normalized echo amplitude variance is 0.025 or smaller. The largest echo variance observed was 0.77. Adaptive beamforming on such a range bin is not fruitful. On the other hand, it is possible to self-cohere the array on the echoes from a low-variance bin and scan the adaptively formed beam at all other ranges. Fig. 3 is an example. There the beam is self-cohered at the range bin used in Fig. 2 and then scanned at the range bin having the 0.77 variance (solid curve). The response of the rigid, electronically scanned phased array is shown dashed. Again the agreement is excellent.

While this experiment has shown that the algorithm works on ground clutter having the proper statistical properties, it has not disclosed the frequency of occurrence of such clutter cells. This knowledge is necessary for system design purposes but unfortunately is not available from the experiment because the transmitting beam of the rigid array was the same width as the receiving beam of the self-cohered array. In contrast, the contemplated airborne radio camera designs use a small, broad-beam transmitter in conjunction with a large, receive-only self-cohered aperture having a very narrow beamwidth [4]. This matter remains to be studied.

References

[1] B. D. Steinberg, E. N. Powers, D. Carlson, B. Meagher, Jr., R. S. Berkowitz, C. N. Dorny and S. Seeleman, "First experimental results from the Valley Forge radio camera program," *Proc. IEEE*, vol. 67, no. 9, pp. 1370–1371, Sept. 1979.

[2] B. D. Steinberg, "Radar imaging from a distorted array: The radio camera algorithm and experiments," to be published in *IEEE Trans. on Ant. & Prop.*, Sept. 1981.

[3] ——, *Principles of Aperture & Array System Design*. New York: Wiley, 1976.

[4] B. D. Steinberg and E. Jadlovker, "Distributed airborne array concepts," to be published in *IEEE Trans. Aerospace Electron. Syst.*

Phase Synchronizing a Nonrigid, Distributed, Transmit-Receive Radar Antenna Array

BERNARD D. STEINBERG, Fellow, IEEE

University of Pennsylvania

A means is described for self-organizing a nonrigid, distributed, transmit-receive antenna array for use in airborne radar. The techniques are applicable to ground-based or shipborne radar as well. Methods are described for initializing the array using various primary microwave illuminators. The description of phase conjugation techniques and means for distributing phase reference to all elements in the array are the central parts of the paper.

Manuscript received October 20, 1981; revised March 15 and April 12, 1982

Author's address: Valley Forge Research Center, The Moore School of Electrical Engineering, University of Pennsylvania, Philadelphia, PA 19104

This work was supported in part by the Air Force Office of Scientific Research and in part by the Office of Naval Research.

0018-9251/82/0900-0609 $00.75

I. INTRODUCTION

An airborne radar with a phased array the size of the aircraft would have many desirable attributes [1]: (1) for fixed transmitter power, the large aperture would provide unusually large detection range; (2) for a given desired performance, the transmitter power could be reduced dramatically; (3) the small horizontal beamwidth would offer a resolving power approaching human vision, which is a few milliradians; (4) adaptive interference cancellation circuits [2-4] operating from the large aperture would suppress jamming very close to the beam axis.

An aircraft-size array would consist of flush-mounted antenna elements distributed throughout the skin of the aircraft. Structural members, doors, windows, etc., would preclude a regular distribution of element locations. Furthermore, the nonrigidity of the airframe and skin would displace the elements from their design positions when in flight. Thus the design principles must be based upon the properties of the random array [5, 6] and self-cohering or adaptive beamforming techniques must be used to compensate for the time-varying positions of the array elements [7-9]. Such a system is called a "radio camera."

Adaptive beamforming is a retrodirective process in which a beam is focused upon a synchronizing source external to the array [10, 11]. The synchronizing source for an airborne radio camera must be another aircraft, a surface target, or clutter [12].

An airborne radio camera can use a conventionally designed transmitter and a distributed receiving array. Alternatively, transmission as well as reception can take place through the self-cohered array. The latter is a much more formidable problem. Means for accomplishing it is the subject of this paper.

The main reason for accepting the increased complexity of the transmit-receive system is because of the poor sidelobe properties of the one-way pattern. The sidelobes of the random array are high because of the random locations of the elements: the average sidelobe level is N^{-1} (N = number of elements) [5] and the peak sidelobe level is 10 dB higher or more [6]. By transmitting through the same array the side radiation pattern is squared, average sidelobe power level (ASL) drops to N^{-2}, and PSL $\approx 100\ N^{-2}$.

Symbols and abbreviations used in this paper are

ASL	average sidelobe power level
BPF	bandpass filter
N	number of elements
PCC	phase conjugating circuit
PLL	phaselock loop
PSL	peak sidelobe power level
VCO	voltage controlled oscillator
VCPS	voltage controlled phase shifter.

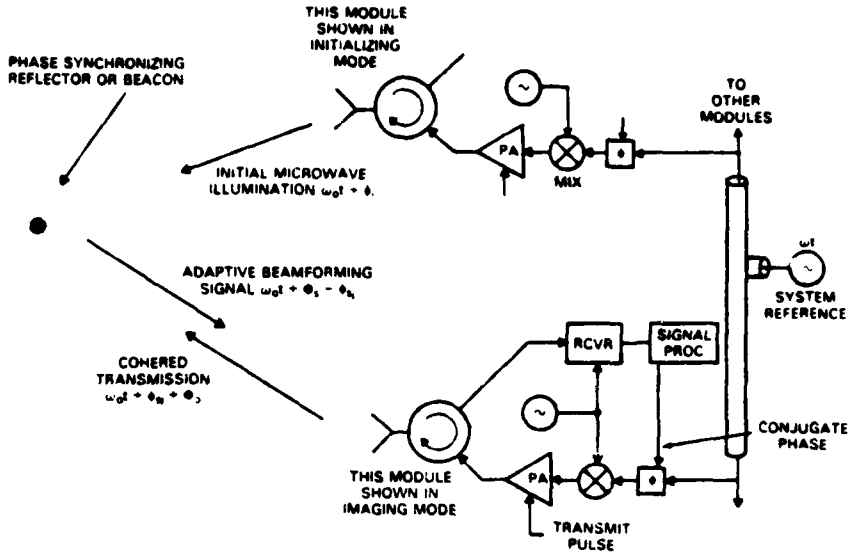

Fig. 1. Adaptive beamforming transmit-receive array without auxiliary transmitter.

II. INITIALIZATION OF THE ARRAY

Synchronization or self-cohering of a random, distorted receiving array has been amply demonstrated [9, 27]. An external reference field is required, as in holography. Measurements of the field disclose the phase corrections to be made at each antenna element. The array is then scanned as a phased array. When transmitting through the same array, however, a logical difficulty is encountered. The external reference field needed to cohere the array must first be set up by the transmitter before the array can be used for transmission.

A variety of techniques can be used to break this conundrum.

(1) The first is to overdesign the transmitter by the necessary margin of N, the number of antenna elements, which is the relative gain of the synchronized array to the nonsynchronized array. This is a costly choice.

(2) Use a separate high gain illuminator for initial synchronization and transfer power to the array afterwards. This is a sound approach when an auxiliary transmitter is available.

The auxiliary radar transmitter could be a nearby radar operating in the same frequency band but not at the same frequency. Target reflections at that frequency can successfully phase synchronize the receiving system. Phase conjugation of the received waveforms results in a receiving beam focused at the source [7-9]. However, since the transmission of the phase-conjugated waves from the antenna elements is at a slightly different frequency, the transmitting beam is offset somewhat, an effect which must be prevented by special phase conjugation circuits of the the type described by Chernoff in [13]. An important advantage is obtained in using a lower frequency for initial synchronization on a target reflection, for then the lobes of the reradiation pattern are widened by the frequency ratio, thereby easing a size-limitation tolerance on the synchronizing source [8]. Instead of a passive source the auxiliary radar could actuate an active beacon which would radiate to the array at the design frequency to self-cohere the array. This avoids the angular offset or "squint."

(3) A rigid subarray of the full system can be used for coherent transmission of a broad beam to establish the reference field.

(4) The entire array can be driven noncoherently prior to self-phasing, in which case the average power density is N^{-1} times the full power density of the system after the array is synchronized. Although this loss is large, it can be compensated through use of a beacon or by initializing on the reflected signal from a nearby target. The squint problem is avoided since synchronization is at the system frequency. The method is effective when synchronizing upon target reflections because of the R^{-4} dependence of received signal power on target distance. To overcome a 30 dB initializing disadvantage ($N = 1000$) the reference reflection must be located no further than 18 percent of the maximum distance at which it could be placed if the transmitters were cohered. This distance reduces to 10 percent when $N = 10^4$. This technique, appropriate for an airborne system using ground or sea clutter for the reference target [12, 28], is illustrated in Fig. 1. Two modules of the array are shown. Each consists of an antenna element, circulator (or other diplexer), receiver, phase-stable reference oscillation common to the entire array, transmitter phase shifter, mixer, local oscillator cohered in frequency to the reference wave, and pulsed power amplifier.

To initialize the system each module radiates an RF pulse having common system frequency ω_0 and random phase. The instantaneous transmission phase of the

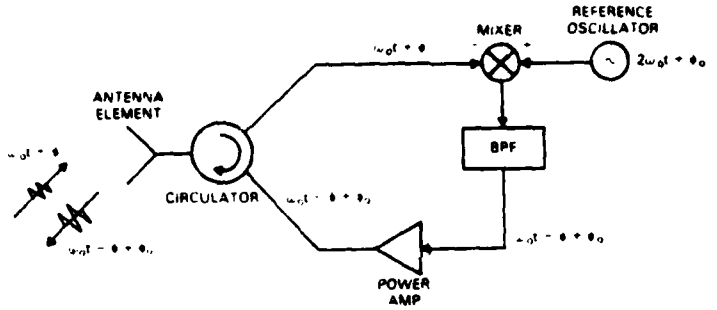

Fig. 2. Phase conjugation schematic.

wave from the ith module may be designated $\omega_0 t + \phi_i$. This wave arrives at the synchronizing source with delay $\omega_0 t + \phi_i - \phi_{i_s}$, where ϕ_{i_s} is the phase delay from the module. The combined illumination at the reflector or beacon is $\sum_{i=1}^{N} a_i \exp j(\omega_0 t + \phi_i - \phi_{i_s})$, the instantaneous phase of which is $\omega_0 t + \Phi_s$, the subscript meaning source. The source wave is returned to the array with a different phase delay ϕ_{s_j} at each module. Thus the signal phase received by the jth module is $\omega_0 t + \Phi_s - \phi_{s_j}$.

To focus the transmitting beam upon the source the radiation from the jth module must be changed from $\omega_0 t + \Phi_s - \phi_{s_j}$ to $\omega_0 t + \phi_{s_j} + \Phi_0$ where Φ_0 is an arbitrary phase constant across the array. This is the phase conjugation step needed to achieve retrodirectivity, which is the heart of the process.

III. PHASE CONJUGATION TECHNIQUES

Retrodirectivity requires phase conjugation at each element, which in turn demands symmetry with respect to some reference. If $\phi_R(x;\theta_0)$ is the phase of the received wave at position x in the array due to a synchronizing source at angle θ_0, and $\phi_T(x;\theta_0)$ is the transmitted phase variation needed to achieve retrodirectivity, the required relation is $\phi_T(x;\theta_0) = -\phi_R(x;\theta_0)$ plus an arbitrary constant. This equation implies the existence of some reference phase from which ϕ_T and ϕ_R may be measured. The symmetry can exist in more than one domain. Spatial symmetry is utilized in one of the oldest forms of retrodirective array, the Van Atta array [14, 15]. Symmetrical sidebands in the frequency domain is another. A third is paired, symmetrical phase shifters.

Dependence upon spatial symmetry is inappropriate for an airborne array distributed about the airframe. Here the array is assumed to be distorted, random, and highly thinned.

The other two techniques are practical. The use of symmetrical sidebands is illustrated in Fig. 2. Let a signal characterized by the real (or imaginary) part of $\exp[j(\omega_0 t + \phi)]$ be received and heterodyned (mixed) with a local oscillator at frequency ω_{LO}. The mixer products are $\exp\{j[(\omega_{LO} + \omega_0)t + \phi]\}$ and $\exp\{j[(\omega_{LO} - \omega_0)t - \phi]\}$. The sidebands are symmetrically displaced about the local oscillator frequency and the lower sideband has the desired phase. Further, if the local oscillator frequency is made exactly twice the frequency of the received signal, the lower sideband is $\exp[j(\omega_0 t - \phi)]$.

In Fig. 2, the input signal at frequency ω_0 and phase ϕ (indicated by the instantaneous phase $\omega_0 t + \phi$) is passed through a circulator where it mixes with the second harmonic at an arbitrary phase ϕ_0. The difference frequency output of the mixer, at ω_0, is passed by the bandpass filter to the amplifier. The phase of this signal is $\omega_0 t + \phi_0 - \phi$. This signal is amplified and radiated. Provided that ϕ_0 is constant across the array, the radiation is retrodirective.

This circuit is useful for illustration but has two limitations which keep it from being a practical circuit. First, the down-converting mixer is a source of trouble because of the harmonic relation between the signals at its inputs. Being a nonlinear circuit the second harmonic of its fundamental frequency input will be generated. A current due to the second harmonic will flow in the source impedance of the second-harmonic input circuit, thereby altering the phase of the reference signal at $2\omega_0$. Also direct feedthrough of the input signal to the output will alter the phase of the output signal. Either the frequency of the reference signal must be different from $2\omega_0$ to avoid these troubles or the mixer must be carefully balanced so that neither second harmonic generation nor input-output leakage will affect the phase of the radiated wave.

The second problem is that this circuit transmits an amplified replica (with conjugated phase) of the received radar trace concurrent in time with the received signal. However, the desired transmission is an RF pulse (with conjugated phase) occurring at a later time. This means that the echo received from the synchronizing source must be sampled, its phase extracted, conjugated and applied to an oscillation at the echo frequency, which is gated at the appropriate time, amplified, and radiated.

Figs. 3-7 show several circuits for accomplishing this task. They differ in their means of storage of the phase information (as the phase of a coherent oscillator, e.g.,

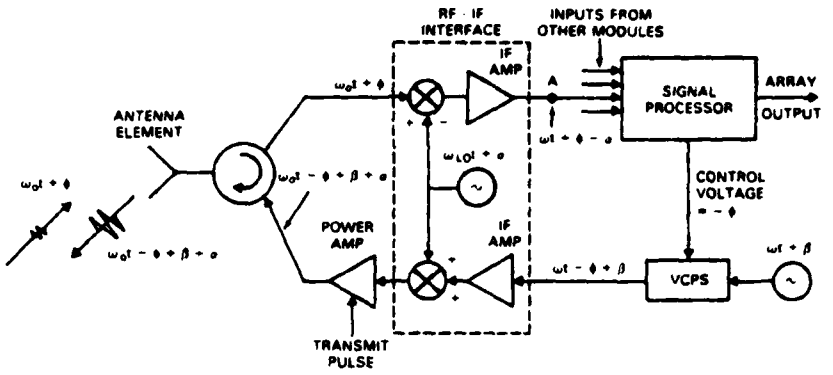

Fig. 3. *Phase conjugation circuit.*

as in a phaselock loop (PLL) [16-21], or as a digital number is the signal processor of the system), according to whether control of the phase shifter through which the signal to be transmitted is passed is open loop or closed loop, and according to the choices of components, e.g., analog versus digital phase shifters.

Fig. 3 shows a means of phase conjugating when a digital signal processor is used to combine the signals received from the distributed array elements. The received signal is shown as an echo pulse having instantaneous phase $\omega_0 t + \phi$. It is heterodyned to IF by a local oscillator at frequency ω_{LO} having some arbitrary phase α. The LO is assumed to be cohered to the reference wave at the intermediate frequency ω. The phase β of the reference is assumed to be constant across the array. The IF pulse, with instantaneous phase $\omega t + \phi - \alpha$, is delivered to the signal processor. The signal processor measures the phase relative to the phase of some reference element in the array, whose phase is arbitrarily identified as zero phase. Since all signals entering the signal processor experience the same phase offset α, the local oscillator phase cancels out. The negative of the measured signal phase ϕ is delivered as a control voltage to a voltage controlled phase shifter (VCPS) in the reference signal path. The output, having instantaneous phase $\omega t - \phi + \beta$, is up converted to form the transmitted wave. The transmitted phase is $\omega_0 - \phi + \beta + \alpha$. Provided that β and α are constants across the array, the transmitted wave is the phase conjugate of the input signal.

The accuracy to which the signal processor measures ϕ (or $-\phi$) is influenced by noise and multipath. However, the precision with which this measurement is made and held for delivery to the phase conjugation circuit can be made arbitrarily fine; it is determined by how many significant figures or bits are used in the measurement. Thus the quality of the delivered value $-\phi$ need be no poorer than that of the measured $+\phi$.

Errors develop when the phase shifts through the system are not tuned out. Let the phase shift be δ from the antennna to the VCPS through the circulator, receiver, and signal processor. The output of the phase shifter then becomes $\omega t - \phi - \delta + \beta$. Let the phase shift be η in the transmitting chain from VCPS to the antenna through the transmitter and circulator. The radiated wave becomes $\omega_0 t - \phi - \delta + \beta + \alpha + \eta$. Its phase is in error by $-\delta + \eta$. The variance of this error (in square radians) across the array, multiplied by 10 log e, is the expected loss in array gain in decibels [12]. For example, 1/4 rad^2 phase error variance leads to a loss in mainlobe gain of 1 dB. Thus each module must be carefully tuned to balance the phase shifts in the receiving and transmitting chains.

The circuit of Fig. 3 stores the signal phase in the signal processor and uses open-loop phase control. The next circuit (Fig. 4) retains open-loop phase control but remembers the signal phase in a PLL. This circuit also demonstrates the use of paired, symmetrical phase shifters. The receiver chain is the same as in Fig. 3 to point A, at which point the circuit branches. The received signal continues to the signal processor as before. It also is applied to the input port of the phase detector in a PLL in which the controlled element is a VCPS rather than the more common voltage-controlled oscillator (VCO). The control voltage in the loop drives the phase of the signal at the VCPS to be in quadrature with the input IF signal. As in the earlier system the signal through the VCPS is the reference oscillation at ω with arbitrary phase β. Hence the loop drives the VCPS to a phase shift $\phi - \alpha - \beta - \pi/2$. Ganged to the VCPS is a matched phase shifter with opposite phase. Its phase is $-\phi + \alpha + \beta + \pi/2$. While the phase of the VCPS is set in a closed loop, the paired phase shifter is set open loop. Carefully matched analog phase shifters are required; otherwise digital phase shifters must be used.

Digital phase shifters generally are preferable. The number of discrete phase-shift components required is easily calculated. If m is the number of quantization bits and M is the number of levels of quantization, the relation between them is given by $M = 2^m$. The loss in gain as a function of the number of quantization bits is [12]

$$\text{loss in gain (dB)} = 20 \log [\sin(\pi/2^m)/(\pi/2^m)]. \quad (1)$$

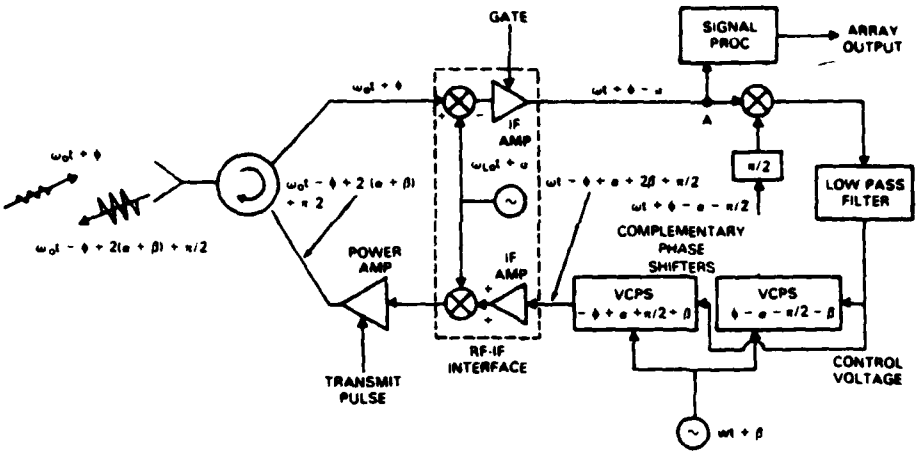

Fig. 4. Phase conjugation circuit.

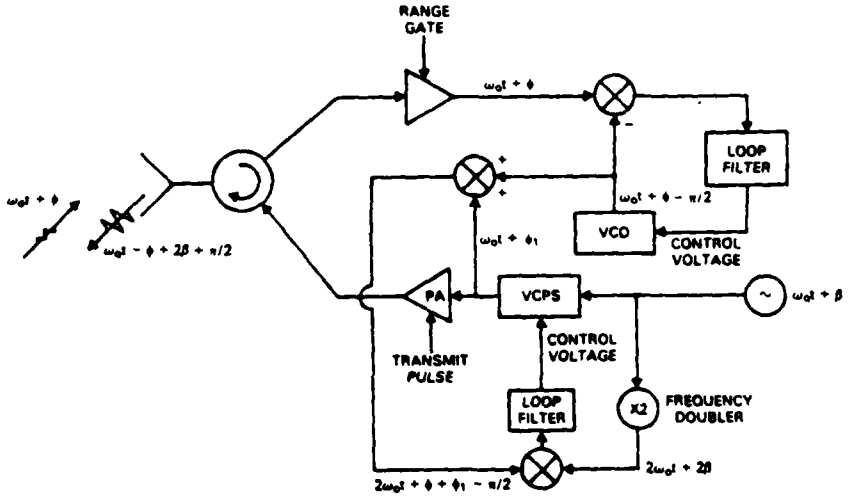

Fig. 5. Phase conjugation circuit.

A quantization value of two bits limits the loss to less than 1 dB, a value of three bits to less then 1/4 dB, and a value of four bits to 0.06 dB. The side radiation pattern also is affected by phase quantization errors, although the statistics in the sidelobe region are not. This is because the element positions are randomized, leading to Rayleigh sidelobe statistics. Further phase errors do not noticeably increase the sidelobe levels; they only reduce the mainlobe gain.

Returning to the figure, it is seen that the input to the paired phase shifter is $\omega t + \beta$; its output, therefore, is $\omega t - \phi + \alpha + 2\beta + \pi/2$. This IF signal is heterodyned to RF via the mixer and the local oscillator at $\omega_{LO}t + \alpha$. The upper sideband at ω_0 is selected by the power amplifier, providing a signal at the desired frequency having a phase $\omega_0 t - \phi + 2(\alpha + \beta) + \pi/2$. This signal is gated in the power amplifier by the transmit-pulse waveform from the radar synchronizer, and radiated. Provided that $\alpha + \beta$ is a constant across the array the high power transmitted pulse has the desired phase.

Fig. 5 shows a phase conjugating circuit (RF-IF heterodyning circuits not shown) which replaces the open-loop ganged phase shifter of Fig. 4 by a phase shift circuit under closed-loop control.[1] The circuit is PLL. The received target echo at $\omega_0 t + \phi$ is applied to the PLL. The VCO phase after the loop is locked is $\omega_0 t + \phi - \pi/2$. It is applied as one input to an up converter. The other input, also at ω_0, is delivered by a voltage controlled phase shifter driven by the reference oscillation. Call its phase ϕ_1. The up converter output is at the second harmonic frequency $2\omega_0$. Its instantaneous phase is $2\omega_0 t + \phi + \phi_1 - \pi/2$. Assume that adequate balance is achieved in the up converter to avoid second harmonic feed through. This signal is compared in a phase detector with the second harmonic of the reference. The beat product is integrated in the loop filter and applied as the

[1]This circuit and the next two were suggested by Prof. Y. Bar-Ness of Tel Aviv University while a Visiting Professor at the University of Pennsylvania.

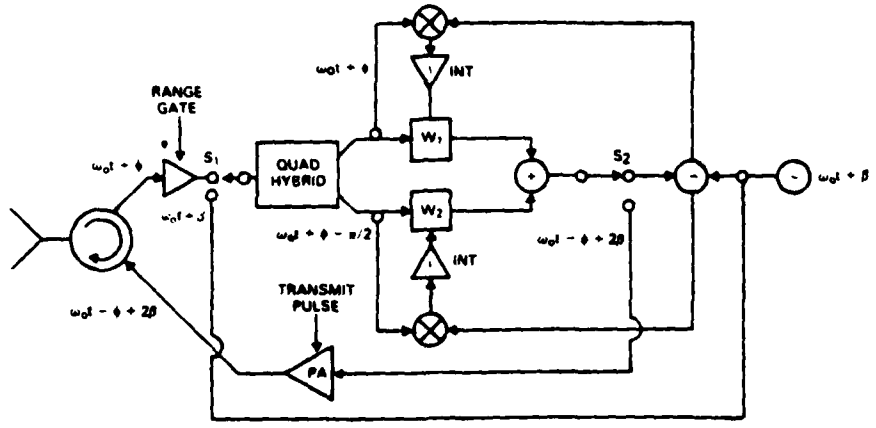

Fig. 6. Phase conjugation (another method).

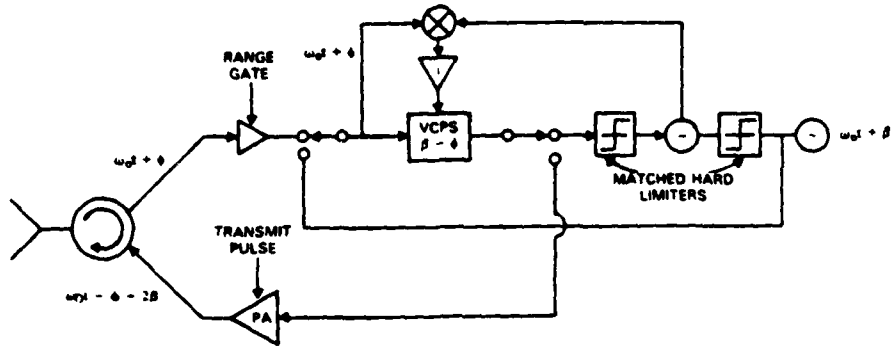

Fig. 7. Hard-limited version of Fig. 6.

control voltage to the VCPS. Convergence requires that $\phi + \phi_1 = 2\beta$ or $\phi_1 = -\phi + 2\beta$. Thus the instantaneous phase of the CW output of the VCPS is $\omega_0 t - \phi + 2\beta$, which is the correct frequency and phase provided that β is constant across the array. Hence the drive for the gated power amplifier is taken from this point.

The circuit of Fig. 6 introduces another method of phase conjugation. The received echo pulse from the reference target is gated as before. The input to the phase conjugating network is switch S_1, connected as shown. The echo at $\omega_0 t + \phi$ passes through a quadrature hybrid which delivers pulses at $\omega_0 t + \phi$ and $\omega_0 t + \phi - \pi/2$. These signals are weighted by real gain controls w_1 and w_2 and added. This sum, $w_1 \cos(\omega_0 t + \phi) + w_2 \cos(\omega_0 t + \phi - \pi/2)$, passes through switch S_2 to the comparator where it is subtracted from the reference wave $\cos(\omega_0 t + \beta)$. The difference is fed back to the mixers of two correlators, the other inputs of which are driven by the quadrature outputs of the hybrid. The integrated mixer products drive the real weights w_1 and w_2 to those values that cause the sum waveform to equal $\cos(\omega_0 t + \beta)$.

The portion of the circuit between the switches is used extensively in adaptive nulling and interference cancellation problems. The closed loops set the weights w_1 and w_2 so as to solve the equation

$$w_1 \cos(\omega_0 t + \phi) + w_2 \cos(\omega_0 t + \phi - \pi/2) = \cos(\omega_0 t + \beta). \tag{2}$$

The solution is

$$\tan(\phi - \beta) = w_2/w_1, \qquad w_1^2 + w_2^2 = 1. \tag{3}$$

When the loops have converged, the circuit between the two switches has transformed the input $\omega_0 t + \phi$ to the output $\omega_0 t + \beta$. In short, the transfer function of the circuit at ω_0 is $H(\omega_0) = \exp[j(\beta - \phi)]$ which means that the circuit is a phase shifter having phase shift $\beta - \phi$. Following loop convergence the weights are frozen and both switches are thrown to their lower positions. The reference wave having phase $\omega_0 t + \beta$ then passes through the circuit and emerges with phase $\omega_0 t - \phi + 2\beta$. It is amplified, gated, and radiated.

Fig. 7 shows another version of the previous circuit in which the signals entering the comparator are hard limited in carefully matched limiters. Given that their amplitudes are matched it is only necessary to shift the

phase of the input echo by $\beta - \phi$ to zero the comparator output. Only a single cancellation loop is needed as there is only a single parameter to be varied. A latching phase shifter, such as the digital phase shifter discussed earlier, is required. After loop convergence is completed the phase shift is frozen, the switches are thrown and $\omega_o t - \phi + 2\beta$ is radiated.

IV. ERRORS IN PHASE CONJUGATION

Two types predominate. The first is a random phase shift due to mistunings in open-loop portions of phase conjugating networks. The second is a linear phase shift due to a frequency offset. The former constitutes a random variation in phase across the array, the effect of which is loss in mainlobe gain as described earlier. Assuming a 1-dB total loss budget for the entire system, the allowed phase error is about 1/2 rad rms. It is evident that the allowed random error in phase conjugation is smaller still. Frequency offset, which has been ignored in the preceding section, may occur in two ways. First, the initializing microwave illuminator may be at a somewhat different frequency from the transmitting array. Second, the need for isolation between low-level incoming signals and high-level outgoing signals may force a frequency offset. The effects are the same in both cases.

The magnitude of the frequency offset is determined by the manner in which the phase is conjugated. The simplest way is to adjust the phase shift at the initial frequency and accept the error which results. Let the reflecting source be at angle $\theta_o = \sin^{-1} u_o$ from the array normal and the initializing (self-cohering on reception) frequency be $\omega' = k'c$. The phase of the wave across the array is $\phi_R = k'xu$. Let $i_0(x)$ be the excitation across the transmitting array. Let the conjugated phase be $-k'xu_0$ and let the wave-number of the signal transmitted by the array be k. The radiation pattern becomes

$$f(u;u_0) = \int i_0(x) \exp(-jk'xu_0) \exp(jkxu)\, dx$$

$$= \int i_0(x) \exp(jkx\{u - [(k'/k)u_0]\})\, dx. \quad (4)$$

Note that the beam no longer points to u_o but to $k'u_o/k$. The error or displacement

$$\Delta u_0 = u_0[1 - (k'/k)] = u_0[1 - (\omega'/\omega)] \quad (5)$$

is called the squint angle. Equation (5) can be rewritten

$$|\Delta u_o/u_o| = |\Delta\omega/\omega| \quad (6)$$

indicating that the magnitude of the fractional change in the beamsteering angle equals the magnitude of the fractional change in the frequency. The largest typical value of $\Delta\omega$ is the receiver bandwidth. Rarely will the angular displacement exceed one or a few percent of the scan angle. Such scale distortion will be unimportant unless the beam displacement exceeds the beamwidth of the large array and no synchronizing source resides within the transmitting beam. A phase conjugating circuit devoid of squint is required if this problem is anticipated [13].

The reason why the angle distortion arises is that the phase is measured and conjugated at one frequency but radiation takes place at another frequency. The error is eliminated if the phase shift resulting from the conjugation process is correct at the new frequency. Then the radiation pattern of the retrodirective array is

$$f(u,u_0) = \int i_0(x) \exp[jk'x(u - u_0)]\, dx f[k'(u - u_0)] \quad (7)$$

The argument of the function is $k'(u - u_o)$. The beamsteering angle, therefore, is u_o. Hence the frequency change is no longer reflected in an angular displacement. The sole effect is a change in the angular scale, measured from u_0, by a factor k'/k. This scale change is of no consequence in adaptive beamforming.

V. PHASE REFERENCE

A reference oscillation with constant phase $\omega t + \beta$ is required in every module in the array. This signal must be derived from an oscillator arbitrarily located in the array and delivered to each module by a circuit or subsystem. A frequency-stable and phase-stable oscillator is assumed as well as a frequency synthesizer capable of generating the local oscillator waveform.

Cables of equal and constant lengths can deliver the reference wave from the source to each module. This is a practical technique when the array is compact and the modules are contiguous. It becomes impractical when the array is large and distributed. Furthermore, being an open-loop system, differential phase changes between cables due, for example, to temperature differences or mismatches at connections are passed directly as phase errors to the modules.

Circuits have been devised to deliver the phase reference from source to module, or from module to module. The major impetus to date has been design work for the Solar Power Satellite [22, 23]. Fig. 8 illustrates a method due to Lindsey [24]. It consists of two distinct circuits separated by a cable having arbitrary phase delay Δ. The reference signal passes between circuits via this cable at frequency ω. It is provided to each phase conjugating circuit at twice that frequency and at the common reference phase β. Thus in the left circuit of Fig. 8 is a reference source of frequency 2ω and phase β.

The upper left circuit is a PLL. Its VCO phase is $\omega t + \phi_o$ where, for the moment, ϕ_o is an arbitrary value. Oscillator output is taken from the loop and passed, via the first diplexer (shown as a circulator), to the cable, which delivers $\omega t + \phi_o - \Delta$ to the right-hand circuit.

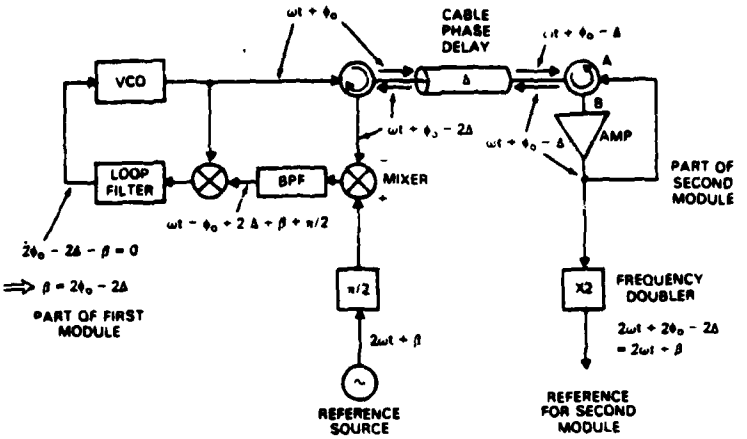

Fig. 8. Frequency and phase-reference delivery circuit (from [24]).

There the cable-delivered signal is doubled in frequency to provide the reference $2\omega + 2\phi_0 - 2\Delta$ for the second module. In this way both modules are driven by the same reference frequency. It is shown below that they are also driven to the same phase.

Prior to frequency doubling in the second module, the amplified wave at $\omega t + \phi_0 - \Delta$ is fed back to the second diplexer and returned to the first module. Its phase is further retarded by the cable delay Δ. It is passed by the circulator to the mixer where it is heterodyned by the 90° phase shifted reference wave. The lower sideband is selected by the bandpass filter (BPF). Its output is the input to the phase detector of the PLL. The instantaneous phase of this wave is $\omega t - \phi_0 + 2\Delta + \beta + \pi/2$. The other input is $\omega t + \phi_0$, delivered by the VCO. The low-pass filtered output of the phase detector is zero when the loop drives the phase difference between the inputs to 90°. Hence $2\phi_0 - 2\Delta - \beta = 0$ or $\beta = 2\phi_0 - 2\Delta$, which is the condition sought. Thus both modules have the same reference phase $2\omega t + \beta$ independent of the cable length between them. Other modules are fed in the same manner.

The circuit as drawn in Fig. 8 is subject to several phase error sources. First, the nonlinear mixer will generate harmonics of the input signal. The second harmonic will add to the reference source at 2ω to produce a net reference signal with altered phase. In addition, feed through the mixer at the fundamental frequency will alter the net phase of the signal delivered by the bandpass filter to the phase detector of the PLL.

The second source of phase errors is the phase shifts through all the nonclosed-loop controlled portions of the circuit. The circulators, the bandpass filter, and the signal return loop are examples. This is a tuning-type problem common to all the preceding circuits as well.

Last, the signal-return loop has a special problem. Unless there is sufficient isolation in the circulator from ports A and B, the loop will oscillate. The amplifier is needed to overcome the signal losses to the cable in both directions. Hence the signal level delivered back to the circulator as port A is larger by the gain of the amplifier than the signal delivered by the circulator at port B. The ideal circulator (or other diplexer) provides zero coupling between ports A and B; the practical circulator has limited isolation. To avoid the danger of oscillation the isolation must exceed the amplifier gain which, in turn, must at least equal the two-way cable loss. Hence the maximum allowed cable loss is limited by the isolation available in practical circulators.

A small modification to the circuit avoids the more serious of these problems. Fig. 9 shows the reference source frequency to be m times the VCO frequency and the frequency of the return signal to be $n\omega$. The VCO signal $\omega t + \phi_0$ again is delivered by cable to the next module, amplified, and returned. The return signal is frequency multiplied by the factor n, delaycd by the cable, and mixed with the reference in the down converter. The phase of the output of the BPF is $(m - n)\omega t + \beta - n\phi_0 + (n + 1)\Delta + \pi/2$.

The VCO output is multiplied in frequency by $(m - n)$ to equate the frequencies of the phase detector inputs. The loop drives these signals into quadrature, resulting in the phase equation $m\phi_0 - \beta - (n + 1)\Delta = 0$, which implies that the instantaneous phase of the reference source $m\omega t + \beta = m\omega t + m\phi_0 - (n + 1)\Delta$.

The output to the next module is derived from a frequency multiplication, by the factor m, of the signal delivered by the cable; its phase is $m\omega t + m\phi_0 - m\Delta$. The only condition required to equate the last two expressions is $m = n + 1$. When this condition is met the desired phase reference is transferred from the first to the second module. In addition, the need for the frequency multiplier (shown dashed) which follows the VCO and drives the phase detector is eliminated; instead a direct connection may be made.

System frequencies are determined by the choice of a

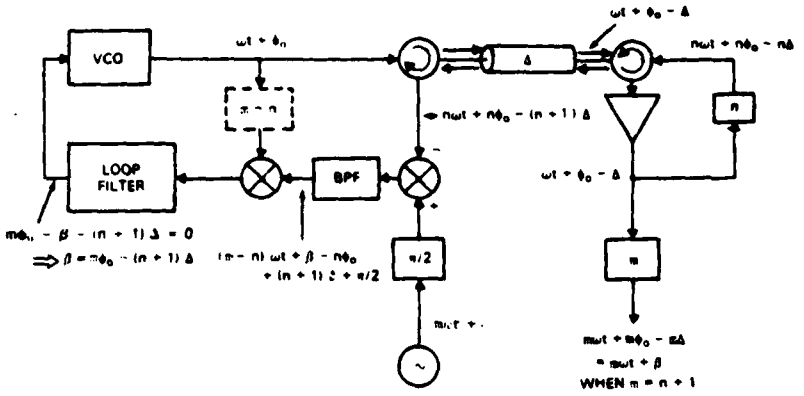

Fig. 9. Improved reference delivery circuit.

convenient VCO frequency ω and the desired frequency offset $\omega(n-1)$. The variable n must be small so that the bandwidths of the circulators and the delay time are not exceeded. n need not be integral; using modern frequency synthesizer techniques frequency multiplication by ratios of integers is easy to obtain. Thus n can be made close to unity. A value of 4/3 permits an adequate frequency separation between the input and the output of the mixer while not requiring excessive bandwidth of the components. The reference phase is delivered at $7\omega/3$ when n equals this value.

VI. EXTERNAL CALIBRATION

Random, uncompensated phase shifts in components throughout the module and the reference-delivery circuits always will exist and will degrade mainlobe gain as indicated in Section III. Periodic calibration or tuning is necessary to limit the loss in mainlobe gain to an acceptable level. Calibration can be manual or automatic in a small system but must be automatic in a system with large array.

A calibration transceiver outside the array can be used for ground-based and shipboard installations. The design of Fig. 10 includes a procedure for correcting the phase of the reference wave at each module and thereby removes the need for a circuit of the type shown in Fig. 9. One module of a distorted array is shown along with the calibration transceiver. Each module has a phase-conjugating circuit (PCC) and a reference wave. Assume that the reference wave is stable in frequency and constant across the array but that the phase varies from module to module. Call the phase of the reference to the ith module β_i, or its total instantaneous phase $\omega t + \beta_i$.

The calibration unit is external to the array and in the general direction toward which the antenna elements are pointed. Its front end consists of a pulsed transmitter and receiver and is similar to the front end of an array module. The reference oscillation in the array is delivered to it either by cable or by radio. The broadcast reference technique [25] is suitable and is the technique illustrated. When the calibration transmitter is connected in the SYNC mode (switches thrown to S), radiation of the system reference at some arbitrary phase from some arbitrary antenna within the array drives the PLL to a frequency ω'. The phase $\omega' t$ of the VCO in the calibration transceiver is the reference phase of the entire system.

After the loop is locked the VCO output is heterodyned to RF and radiated. Its frequency is ω_0, the radiation frequency of the entire system. Since there is some phase shift α from VCO to antenna, the radiated waveform is characterized by $\omega_0 t + \alpha$, as indicated next to the symbol (1) in the figure. The system calibrates one module at a time. The system controller (i.e., the central computer) turns on each module in sequence. Upon arrival of the radiated signal (1) at the antenna of the ith module (2) the phase is $\omega_0 t + \alpha - \phi_i$, where ϕ_i is the propagation phase delay. The phase shift through the antenna in the direction toward the calibration system is γ_i. Since the phase of the element pattern may be different in the direction to the target, γ_i is explicitly retained in this description of system operation. Thus the signal phase after the antenna is $\omega_0 t + \alpha - \phi_i + \gamma_i$. Similarly, there is a phase shift δ_i to the input (4) to the PCC, where the phase is $\omega t + \alpha - \phi_i + \gamma_i + \delta_i$.

The primary reference oscillator of the system runs freely at frequency ω delivering $\omega t + \beta_i$ to the input (5) to a digital shifter ϕ_c. The initial phase shift is some arbitrary value θ_i, making the input reference phase (6) to the PCC $\omega t + \beta_i + \theta_i$. The output (7) of the PCC is

$$\text{phase (7)} = \omega t + \beta_i + \theta_i - [(\alpha - \phi_i + \gamma_i + \delta_i) - (\beta + \theta_i)] = \omega t + 2\beta_i + 2\theta_i - \alpha + \phi_i - \gamma_i - \delta_i.$$

After the wave is heterodyned to RF and passed through the transmitter, its phase (8) is increased by η_i to

$$\text{phase (8)} = \omega t + 2\beta_i + 2\theta_i - \alpha + \phi_i - \gamma_i - \delta_i + \eta_i.$$

γ_i is added through the antenna (9) and the propagation

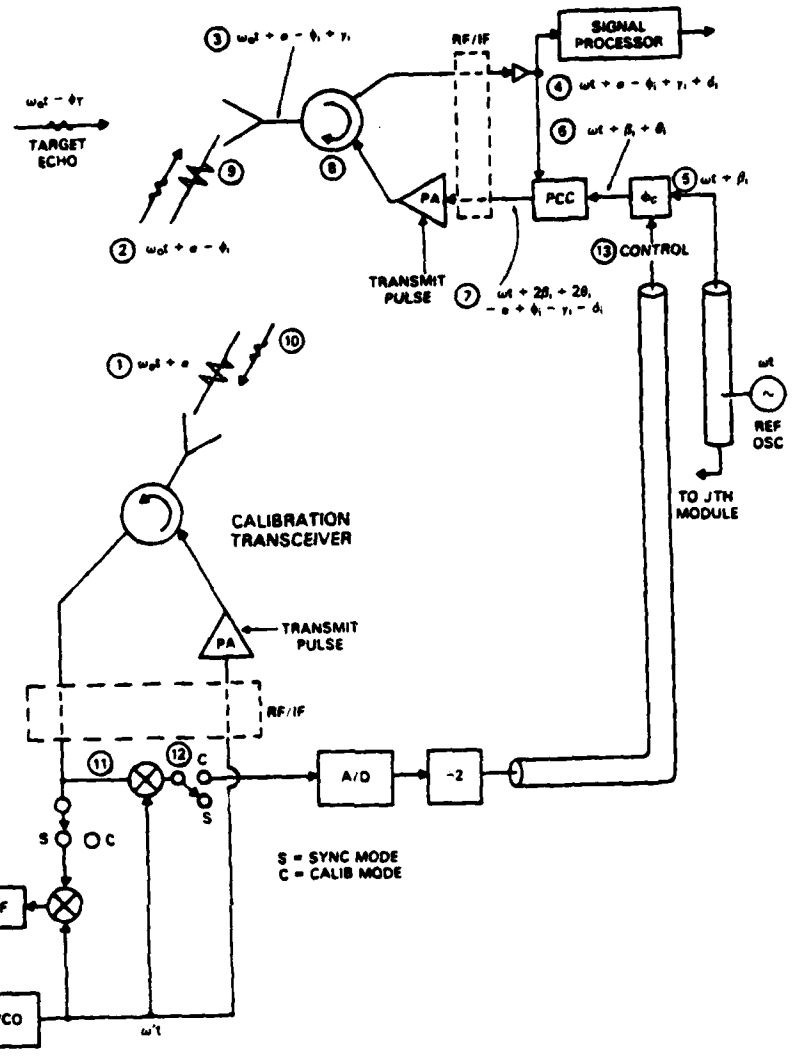

Fig. 10. ith module of distorted array.

delay ϕ_i is contributed upon arrival at the calibration system (10). There the instantaneous phase is $\omega t + 2\beta_i + 2\theta_i - \alpha - \delta_i + \eta_i$. It is evident that both the propagation delay and the antenna element phase shifts have dropped out.

This wave is received with the switches thrown to C, which places the calibration transceiver in the CALIB mode. The phase shift from antenna to phase detector (11) is μ. Hence the phase detector output (12) is a video voltage proportional to $-2\beta_i - 2\theta_i + \alpha + \delta_i - \eta_i - \mu$. This voltage is converted to a digital number, divided by two, and delivered (13) to the digital phase shifter in the module where it changes the phase through that component by $\Delta\phi_c = -\beta_i - \theta_i + (\frac{1}{2})(\alpha + \delta_i - \eta_i - \mu)$. The signal recentering the PCC as a phase reference is, therefore, $\omega t + (\frac{1}{2})(\alpha + \delta_i - \eta_i - \mu)$.

This is the desired reference phase: the random initial phase θ_i of the phase shifter and the random reference oscillation phase β_i have been removed, the circuit phase shifters δ_i and η_i cancel out during system operation (see below), and the remainder is a constant across the array.

Now let a target echo $\omega_0 t - \phi_{T_i}$ arrive at the ith antenna element. The IF signal delivered to the PCC is $\omega t - \phi_{T_i} + \gamma_{T_i} + \delta_i$. The phase-conjugated output is $\omega t + (\frac{1}{2})(\alpha + \delta_i - \eta_i - \mu) - [(-\phi_{T_i} + \gamma_{T_i} + \delta_i) - (\frac{1}{2})(\alpha + \delta_i - \eta_i - \mu)] = \omega t + \alpha - \eta_i - \mu + \phi_{T_i} - \gamma_{T_i}$, and the signal radiated in the direction of the target is $\omega_0 t + \alpha - \mu + \phi_{T_i}$, which is exactly the conjugated phase plus an arbitrary constant.

The only circuit in the system not under closed-loop control is the phase measuring and phase control branch (12) to (13) from calibrator to module. Gain and bias errors can develop in this circuit. Let the phase detector gain be in error by the factor K and let a bias M develop in its output circuit. Then the phase shift in the digital phase shifter is changed by $\Delta\phi_c = K[-\beta_i - \theta_i + (\frac{1}{2})(\alpha + \delta_i - \eta_i - \mu)] + M$. The reference for the PCC becomes $\omega t + \beta_i + \theta_i + \Delta\phi_c \triangleq \omega t + \psi$. The PCC output is $\omega t + 2\psi + \phi_{Ti} - \gamma_{Ti} \delta_i$. After passage through the transmitter and antenna the radiated wave toward the target is

$$\omega_0 t + 2\psi + \phi_{T_i} - \delta_i + \eta_i$$

$$= \omega_0 t + 2M + K(\alpha - \mu) + \phi_{T_i}$$

$$+ (1 - K)(2\beta_i + 2\theta_i + \eta_i + \delta_i). \quad (8)$$

The first four terms are the conjugated phase (ϕ_{T_i}) plus an arbitrary constant ($2M + K(\alpha - \mu)$). The last term represents a phase error in transmission from the *i*th module, which goes to zero when the gain error goes to zero. The maximum effect is easily calculated. β, θ, η, and δ may be assumed to be random variables independent of the errors in the other modules. Their sum is a random phase error. The magnitude of the net phase error ϕ_i is a function of the fractional gain error K of the phase detector. Note that the phase error is not a function of the bias error of the phase detector.

Using the theory of mainlobe gain-loss referenced in Section III [12], a tolerance can be calculated for the phase detector gain error. The random phase error is, at worst, uniformly distributed to the interval $[-\pi, \pi]$.[2] The variance of a uniform distribution is one-twelfth the square of the length of the interval.[3] Hence

$$\sigma_\phi^2 \leq (1 - K)^2 (2)^2/12 \quad (9)$$

which must not exceed 1/4 rad^2 if the loss in mainlobe gain is to be limited to 1 dB. Taking this value as the tolerance in gain loss, the allowed fractional gain error K in the phase detector is found by equating (9) to 0.25, which yields $K = 0.724$. In other words the gain can change by 27 percent without causing more than 1 dB loss in system performance. This is a relatively easy tolerance to maintain.

VII. SUMMARY

The logical requirements for a self-adaptive, nonrigid, distributed radar antenna array are discussed. A transmitter is required to illuminate a target, the reflections from which are received by the elements in the array. The target must reradiate a nearly spherical wavefront. The phases of the received echoes are used to set the phase shifts in the antenna elements so that a receiving beam is focused on the target. The same phase information permits setting the transmission phase shifts as well.

Once the transmitting beam is formed and focused on the target the initializing illumination no longer is required. The beam is scanned by modifying the phase shifts in the same manner that is used in a conventional phased array.

Phase conjugation of the received wave at every element is necessary to achieve focused transmission. There are two primary circuit and system choices to make in the design of phase conjugating networks. The first choice is between analog and digital circuits. The second choice is between open-loop and closed-loop control of the phase shift. The bases for these choices are discussed and several circuits are given. The phase conjugating circuit at each antenna element requires a reference wave of constant frequency and fixed phase. Methods for distributing the phase reference across the array are described.

[2] For example, the probability density function of the modulo-2π sum of two random variables, each uniformly distributed in a 2π interval, also is uniform in the interval. This case corresponds to the equality condition in (9). If the pdfs are clustered near the center of the interval, the pdf of the sum also is clustered, leading to the strict inequality in (9). The random variables in (8) will generally correspond to this case. If the pdfs are lower in the central region than at the edges, the inequality could reverse. There is no physical basis for assuming that this situation will occur in this system.

[3] Let $w(x) = 1/L$, $|x| \leq L/2$ and $= 0$, elsewhere. Then $\sigma_x^2 = (1/L) \int_{-L/2}^{L/2} x^2\, dx = L^2/12$.

REFERENCES

[1] Steinberg, B.D., and Yadin, E. (1982)
Distributed airborne array concepts.
IEEE Transactions on Aerospace and Electronic Systems, Mar. 1982, *AES-18*, 219-227.

[2] Applebaum, S.P. (1966)
Adaptive arrays.
Syracuse University Reasearch Corp., Report STLSPL TR 66-1, Aug. 1966.

[3] Widrow, B., et al. (1967)
Adaptive antenna systems.
Proceedings of the IEEE, Dec. 1967, *55*, 2143-2159.

[4] Brennan, L.E., and Reed, I.S. (1973)
Theory of adaptive radar.
IEEE Transactions on Aerospace and Electronic Systems, Mar. 1973, *AES-9*, 237-252.

[5] Lo, Y.T. (1964)
A mathematical theory of antenna arrays with randomly spaced elements
IRE Transactions on Antennas and Propagation, May 1964, *AP-12*, 257-268.

[6] Steinberg, B.D. (1972)
The peak sidelobe of the phased array having randomly located elements.
IEEE Transactions on Antennas and Propagation, Mar. 1972, *AP-20*.

[7] Steinberg, B.D. (1973)
On the design of a radio camera for high resolution in microwave imaging.
Journal of the Franklin Institute, Dec. 1973.

[8] Steinberg, B.D. (1980)
High angular microwave resolution from distorted arrays.
Proceedings of the Symposium of the Society of Photo-Optical Instrumentation Engineers, Apr. 1980.

[9] Steinberg, B.D. (1981)
Radar imaging from a distorted array: The radio camera algorithm and experiments.
IEEE Transactions on Antennas and Propagation, Sept. 1981.

[10] *IEEE Transactions on Antennas and Propagation*, (Special Issue on Active and Adaptive Antennas), Mar. 1964, *AP-12*, 140-246.

[11] Hansen, R.C. (Ed.) (1964)
Microwave Scanning Antennas, vol 3.
New York: Academic Press, 1964, ch. 5.

[12] Steinberg, B.D. (1976)
Principles of Aperture and Array System Design.
New York: Wiley, 1976.

[13] Chernoff, R. (1979)
Large active arrays for space applications.
IEEE Transactions on Antennas and Propagation, July 1979, *AP-27*, 489-496.

[14] Sharp, E.D., and Diab, M.A. (1960)
Van Atta reflector array.
IRE Transactions on Antennas and Propagation, July 1960, *AP-8*, 436-438.

[15] Hansen, R.C. (1961)
Communications satellites using arrays.
Proceedings of the IRE, June 1961, *49*, 1066-1074.

[16] Gardner, F.M. (1979)
Phaselock Techniques, 2nd ed.
New York: Wiley, 1979.

[17] Viterbi, A.J. (1966)
Principles of Coherent Communication.
New York: McGraw-Hill, 1966.

[18] Lindsey, W.C. (1972)
Synchronization Systems in Communications and Control.
Englewood Cliffs, N.J.: Prentice-Hall, 1972.

[19] Klapper, J., and Frankle, J.T. (1972)
Phase-Locked and Frequency Feedback Systems: Principles and Techniques.
New York: Academic Press, 1972.

[20] Lindsey, W.C., and Tausworthe, R.C. (1973)
Bibliography of the theory and application of the phase-lock principle
Technical Report 32-1581, Jet Propulsion Laboratory, California Institute of Technology, Pasadena, Apr. 1973.

[21] Grimberg, E., and Bar-Ness, Y. (1979)
Acquisition behavior of pulse tracking phase-locked loop.
International Journal of Electronics, July 1979, *47*, 1-15.

[22] Glazer, P. (1968)
Power from the sun: Its future.
Science, Nov. 1968, *162*, 857-861.

[23] Satellite power systems — Concept development and evaluation program.
USDOE and NASA Report DOE/ER-0023.
Available from *National Technical Information Services*, U.S. Department of Commerce, Jan. 1979.

[24] Lindsey, W.C., and Kantek, A.V. (1978)
Automatic phase control in solar power satellite systems.
Technical Report TR-7802-0977, LinCom Corp., P.O. Box 2793D, Pasadena, Calif., Feb. 1978.

[25] Steinberg, B.D., and Powers, E.N (1975)
High angular resolution radar.
Proceedings of the IEEE International Radar Symposium, Arlington, Va., Apr. 1975.

[26] Godlove, T.F., and Granatstein, V.L. (1977)
Relativistic electron beam sources.
Society of Photo-Optical Instrumentation Engineers, *105*, Far Infrared/Submillimeter Wave Technology/Applications, 1977.

[27] Steinberg, B.D. (1982)
Adaptive microwave holography.
Optica Acta, Apr. 1982.

[28] Steinberg, B.D., and Yadin, E. (1982)
Radio camera experiment with airborne radar data.
Proceedings of the IEEE (Letters), Jan. 1982, *70*, 96-98.

Bernard D. Steinberg (S'48—A'50—SM'64—F'66) was born in Brooklyn, N.Y., in 1924. He received the B.S. and M.S. degrees in electrical engineering from the Massachusetts Institute of Technology, Cambridge, in 1949, and the Ph.D. degree from the University of Pennsylvania, Philadelphia, in 1971.

He worked in the Research Division of Philco through the middle 1950's, specializing in radar backscatter and radar signal processing. He was one of the founders of General Atronics Corporation in Philadelphia in 1956 and served as its Vice President and Technical Director for 15 years. His work there was in signal processing techniques and their applications to radar, HF communications, hydroacoustics, and seismology. His most recent work is in self-adaptive signal processors, particularly in large antenna arrays. Since 1971, he has been a Professor with the Moore School of Electrical Engineering at the University of Pennsylvania, Philadelphia, and Director of its Valley Forge Research Center, where he is engaged in development of a large self-adaptive microwave imaging system called the "radio camera." He is the author of *Principles of Aperture and Array System Design* (Wiley, 1976) in which early radio camera concepts are described and currently is preparing a detailed book on the subject. He also is a consultant in the Airborne Radar Branch of the Naval Research Laboratory.

Dr. Steinberg is a member of U.S. Commissions B and C of the International Scientific Radio Union (URSI).